

A HIGH TEMPERATURE VAPORIZATION STUDY
OF SOME GROUP IVb, Vb AND VIb
TRANSITION METAL SELENIDES

A Thesis

Presented to

The Faculty of Graduate Studies and Research
The University of Manitoba

in Partial Fulfilment
of the Requirements for the Degree

Master of Science

by

Alan C. Blizzard

September, 1967

ACKNOWLEDGEMENTS

I should like to thank Dr. J. B. Westmore, my research supervisor, for his advice and encouragement throughout this project.

I also wish to thank the technical staff of the Chemistry and Physics Departments for constructing much of the apparatus and Dr. H. Gesser for suggesting parts of the design.

ABSTRACT

The compounds TiSe_2 , VSe_2 , Cr_2Se_3 , ZrSe_2 , MoSe_2 , TaSe_2 and WSe_2 were studied by effusion cell and free vaporization experiments performed with a continuously recording vacuum thermobalance. The construction of the balance is described in detail. The following thermal stabilities were measured in a vacuum of 10^{-4} mm. Hg: 900°C for MoSe_2 , 750°C for WSe_2 , 640°C for Cr_2Se_3 , 150°C for VSe_2 , ZrSe_2 and TaSe_2 , and 140°C for TiSe_2 . In each case, the decomposition reaction produced gaseous selenium and a solid residue. The identity of the condensed phases formed is discussed with respect to the phases which have previously been reported in each of the metal-selenium systems. Evidence was found for the existence at 1000°C and 10^{-4} mm. Hg of a number of low selenides of tungsten, including W_2Se , which have not previously been reported.

TABLE OF CONTENTS

	Page
INTRODUCTION	
Part One: General Introduction	2
Part Two: Selenides of the Group IVb, Vb, and VIb Transition Metals	4
A. Methods of Preparation	4
B. Crystal Structures	8
C. Established Phases	14
D. Thermal Properties	17
Part Three: Principles of Thermogravimetric Analysis	37
A. Qualitative Analysis	37
B. Vapor Pressure Measurement	42
APPARATUS AND PROCEDURE	
Part Four: Introduction	55
Part Five: Construction and Operation of T.G.A. Apparatus	56
A. General	56
B. Weight Measurement	56
C. Temperature Control and Measurement	73
D. Pressure Control and Measurement	79
Part Six: Experimental Procedure	82
A. General	82
B. Calibration of the Thermobalance	82
C. Thermogravimetric Experiments	89
RESULTS	
A. General	97
B. Minimum Heating Rate Experiments	97
C. Linear Heating Rate Experiments	101

Page

DISCUSSION

A. General.	122
B. Thermal Stabilities.	123
C. Decomposition Reactions.	124

CONCLUSIONS

BIBLIOGRAPHY

LIST OF FIGURES

Figure		Page
1	THE NICKEL ARSENIDE STRUCTURE (a) General view (b) Unit cell	11
2	THE NICKEL ARSENIDE STRUCTURE Projections on the $y = 0$ and $z = 0$ planes	13
3	STRUCTURES RELATED TO THE NICKEL ARSENIDE TYPE (a) The Ni_2In type (b) The $Cd(OH)_2$ type	16
4	TRANSITION METAL-SELENIUM SYSTEMS One dimensional composition diagrams	31
5	TEMPERATURE ERRORS IN A CHEVENARD THERMOBALANCE Temperature lag of sample holder with respect to furnace temperature (a) Effect of heating rate (b) Effect of sample	41
6	THERMOGRAVIMETRIC APPARATUS General arrangement of components	58
7	THERMOGRAVIMETRIC APPARATUS The spring balance	60
8	THERMOGRAVIMETRIC APPARATUS Cross sectional view of the L.V.D.T. assembly	64
9	THERMOGRAVIMETRIC APPARATUS Overall circuit diagram	68
10	THERMOGRAVIMETRIC APPARATUS L.V.D.T. amplifier-rectifier circuits (a) 12 volt power supply (b) 60 Hz amplifier and rectifier	71
11	THERMOGRAVIMETRIC APPARATUS Sample holders (a) Open cell - quartz or "Vycor" brand glass (b) Knudsen cell - stainless steel (c) Knudsen cell - compressed boron nitride	75
12	THERMOGRAVIMETRIC APPARATUS Construction of the furnace	78

Figure		Page
13	L.V.D.T. RESPONSE CURVE Output voltage vs. core position	85
14	L.V.D.T. RESPONSE CURVE CLOSE TO NULL POSITION Output voltage vs. core position	88
15	FURNACE TEMPERATURE PROGRAMS (a) Minimum heating rate (b) Maximum heating rate (c) Linear heating program	91
16	FREE VAPORIZATION OF $TiSe_2$ IN VACUUM (a) Weight vs. temperature at $5.85^\circ C/min.$ (b) Weight vs. time at $1000^\circ C$	103
17	FREE VAPORIZATION OF VSe_2 IN VACUUM (a) Weight vs. temperature at $5.85^\circ C/min.$ (b) Weight vs. time at $1000^\circ C$	105
18	FREE VAPORIZATION OF Cr_2Se_3 IN VACUUM (a) Weight vs. temperature at $5.85^\circ C/min.$ (b) Weight vs. time at $1000^\circ C$	107
19	FREE VAPORIZATION OF $ZrSe_2$ IN VACUUM (a) Weight vs. temperature at $5.85^\circ C/min.$ (b) Weight vs. time at $1000^\circ C$	109
20	FREE VAPORIZATION OF $MOSe_2$ IN VACUUM (a) Weight vs. temperature at $5.85^\circ C/min.$ (b) Weight vs. time at $1000^\circ C$	111
21	FREE VAPORIZATION OF $TaSe_2$ IN VACUUM (a) Weight vs. temperature at $5.85^\circ C/min.$ (b) Weight vs. time at $1000^\circ C$	113
22	FREE VAPORIZATION OF WSe_2 IN VACUUM (a) Weight vs. temperature at $5.85^\circ C/min.$ (b) Weight vs. time at $1000^\circ C$	115
23	CORRECTION FOR DRIFT IN WEIGHT READING (a) Weight vs. temperature at $5.85^\circ C/min.$ (b) Weight vs. time at $1000^\circ C$	117
24	POSTULATED DECOMPOSITION REACTIONS Apparent changes in composition shown in relation to phases previously reported	125
25	VAPOR PRESSURE OF SELENIUM Log P vs. $1/T^\circ K$ extrapolated to 10^{-4} mm. Hg.	129

LIST OF TABLES

Table		Page
1	REPORTED PHASES IN SOME TRANSITION METAL- SELENIUM SYSTEMS	
	(a) The Ti-Se System	18
	(b) The V-Se System	20
	(c) The Cr-Se System	21
	(d) The Zr-Se System	22
	(e) The Nb-Se System	23
	(f) The Mo-Se System	25
	(g) The Hf-Se System	26
	(h) The Ta-Se System	27
	(i) The W-Se System	28
	(j) The Re-Se System	29
2	OXIDATION OF Zr SELENIDES IN AIR	34
3	RESULTS OF MINIMUM HEATING RATE EXPERIMENTS Effusion cell experiments except as noted. All in vacuum.	99
4	RESULTS OF LINEAR HEATING RATE EXPERIMENTS Free vaporizations in vacuum	120

To My Wife

INTRODUCTION

PART ONE: GENERAL INTRODUCTION

This study is an investigation of the compounds: TiSe_2 , VSe_2 , Cr_2Se_3 , ZrSe_2 , MoSe_2 , TaSe_2 and WSe_2 with the object of determining the nature of the vaporization process which each undergoes and, since it appears that they all decompose on heating, their relative thermal stabilities. An attempt is also made to obtain quantitative information in the form of vapor pressures and thermodynamic properties.

A number of recent reviews⁽¹⁻⁸⁾ have amongst them discussed the selenides of rhenium and of all the transition metals of groups IVb, Vb, and VIb. These reviews indicate that interest in these compounds is principally due to their properties as semi-conductors, their low coefficients of friction and their crystallographic properties as examples of the nickel arsenide (NiAs) type of structure. The nature of these interests, and the fact that there are in general a number of different solid phases in each of the metal-selenium systems, have meant that most of the studies of these compounds have been confined to establishing their existence, composition and crystal structure. Studies of their properties have concentrated on thermoelectric and frictional properties rather than thermodynamics.

Information about the thermodynamic properties of these compounds is important for both theoretical and

applied interests. The metal-selenium systems cannot be properly described until the variation with temperature and pressure of their composition is known and full use of their frictional and electrical properties requires a knowledge of their stability under a variety of conditions.

Part two of this introduction contains a summary of the preparative, structural and thermodynamic information which has been published on the selenides of rhenium and the group IVb, Vb and VIb transition metals. Part three is a discussion of the principles of qualitative and quantitative thermogravimetric analysis, the principle experimental techniques used in the present study.

PART TWO: SELENIDES OF THE GROUP IVb, Vb and VIb
TRANSITION METALS

A. METHODS OF PREPARATION

The compounds are most commonly prepared by direct synthesis from the elements. However, a number of indirect methods have been reported which are primarily of historical interest. Transport reactions have been used recently to prepare single crystals for accurate X-ray analysis and for study of magnetic and electrical properties.

A typical procedure for direct synthesis is that described by Bernusset⁽⁹⁾ for the preparation of Ti selenides. A mixture of very pure Ti and Se of the desired stoichiometry is weighed into a quartz tube. The tube is evacuated, sealed, heated to 500° C for one day, and then heated to 1100° C for a minimum of five days to form the product. The tube is quenched in ice-water, opened and the product ground, remixed, heat treated again for a short time and then quenched. The compound is removed from the tube as a compact mass having a metallic lustre.

Variations from this procedure usually involve the temperature and time of heating and the rate of cooling to room temperature. Column three of Table 1 (see page 18) contains the temperatures at which many of the reported compounds were prepared, the length of time for which the reactants are heated is usually of the order of several days

and in order to prepare a phase which is stable at low temperature, annealing for long periods at the temperature of interest is necessary.

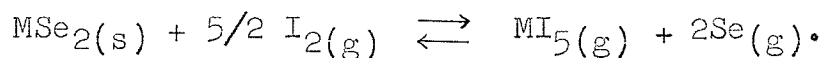
When he used the procedure detailed above, Bernusset found that Ti_2O_3 and Ti_5Si_3 were present in the product, presumably formed by reaction with the quartz reaction tube. The same author previously reported⁽¹⁰⁾ that SiO_2 boats were attacked during preparation from the elements of titanium selenides which are high in titanium content, a mixture of Ti_2O_3 , Ti_5Si_3 and α -cristobalite being formed. Carpay⁽¹¹⁾ found, during the direct preparation of vanadium selenides, that the silica tubes he was using were attacked, especially by vanadium-rich compositions, and the products appeared to contain V_3Si . He was able to avoid this by coating the tubes with graphite. After reactions in coated tubes he found that neither the graphite nor the silica had been attacked.

A direct synthesis without the use of vacuum was reported by Von Bolton⁽¹²⁾. He prepared the selenides of niobium and tantalum by heating a mixture of equal parts of the elements under a layer of fused potassium chloride.

Transport reactions have been used to prepare single crystals for detailed studies of X-ray diffraction patterns and thermoelectric properties. Brixner⁽¹⁾ has used transport reactions to prepare single crystals of the diselenides of niobium, tantalum, molybdenum and tungsten,

Schäfer and Fuhr⁽¹³⁾ a number of niobium selenides and Brown and Beerntsen⁽¹⁴⁾ the diselenides of niobium and tantalum.

Brixner's method was to take five or ten grams of a diselenide produced by direct synthesis from the elements and place it in a quartz tube with one to three milligrams of iodine in the case of niobium, tantalum and tungsten or bromine in the case of molybdenum. The quartz tube was placed in a double wound one inch diameter furnace. With one end at 900° C and the other at 700° C, transport proceeded from the hot to the cold end according to a reaction which Brixner suggests was probably:



The only metal which apparently did not form a volatile iodide under the reaction conditions was molybdenum.

Brixner suggests the transport with bromine probably took place via $MoBr_3$ or $MoBr_4$. Quantities up to ten grams could be transported during ten to fifteen hours. The brightly shining crystals with edges up to five millimeters had the shape of flat, hexagonal plates.

Although direct synthesis from the elements seems to be preferred for the preparation of very pure samples of these selenides, a number of indirect syntheses have been reported. $TiSe_2$, $ZrSe_2$ and $HfSe_2$ have been prepared by passing the vapor of the metal chloride and selenium over a

heated tungsten filament^(15, 16), WSe_3 and MoSe_3 by passing hydrogen selenide through an acidified tungstate or molybdate solution respectively⁽¹⁷⁾, Mo_2Se_5 by reducing a sulfuric acid solution of ammonium molybdate with zinc then saturating it with hydrogen selenide⁽¹⁸⁾, Mo_2Se_3 by fusing MoO_2 and selenium with potassium carbonate at a temperature above 1200°C followed by leaching with water⁽¹⁸⁾, CrSe and Cr_2Se_3 by heating chromous chloride and chromic chloride respectively in a stream of hydrogen selenide⁽¹⁹⁾ and ReSe_2 by the reaction of ammonium perrhenate and hydrogen selenide at 700°C ⁽²⁰⁾. It has been suggested⁽⁷⁾ that transition metal selenides might be synthesized by reaction of the metal hydrides or the metals with selenium or hydrogen selenide since it has been shown⁽²¹⁾ that the reaction between ThH_4 and hydrogen sulfide can be controlled to yield any desired sulfide. Such a synthesis has already been reported⁽²⁰⁾ for ReSe_2 , prepared from the metal and hydrogen selenide.

In some cases, higher or lower selenides have been obtained from a previously prepared selenide by thermal degradation or reaction with the metal, selenium, or hydrogen. For example ZrSe_2 has been prepared by thermal degradation of ZrSe_3 at 900°C ⁽⁴⁾, niobium and tantalum diselenides heated with excess selenium form phases of the type $\text{M}_{1-x}\text{Se}_2$ ($0 \leq x \leq 1$)⁽²²⁾, MoSe_3 when heated to dull red

with selenium and hydrogen forms MoSe_2 ⁽¹⁸⁾ and CrSe may be prepared by heating Cr_2Se_3 in hydrogen⁽¹⁹⁾.

B. CRYSTAL STRUCTURES

All of the compounds investigated in this study and most of the other phases in each of the metal-selenium systems crystallize in forms related to the nickel arsenide (NiAs) type structure. Furthermore, this type of structure is virtually only found in compounds formed by the combination of transition metal atoms with metalloid (i.e., Group IVa, Va and VIa) atoms and provides a means of relating the wide variety of stoichiometric formulae of the phases in which they exist. Therefore, although the present study is not primarily concerned with the crystallographic structure of the compounds investigated, it seems appropriate to describe the main features of the NiAs type structure.

The NiAs type of crystal structure is well known and has been described in detail^(3,23). The description here will be limited to an account of how the structure can be used to describe a wide variety of stoichiometric formulae and an indication of how the frictional properties of NiAs-type compounds may be related to their structure.

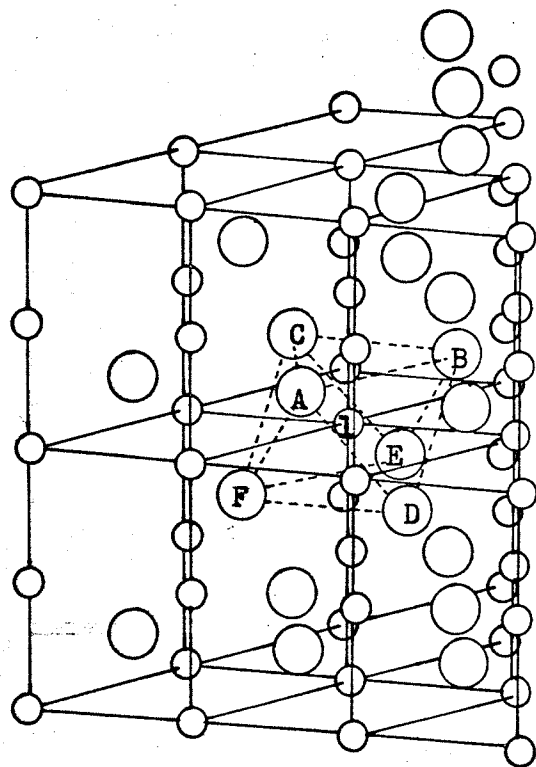
The NiAs structure is represented in figure 1a with an enlarged unit cell shown in figure 1b. Transition metal atoms and metalloid atoms lie on interpenetrating sublattices which are simple hexagonal and hexagonal close-packed structures

FIGURE 1

THE NICKEL ARSENIDE STRUCTURE

- (a) General view
- (b) Unit cell

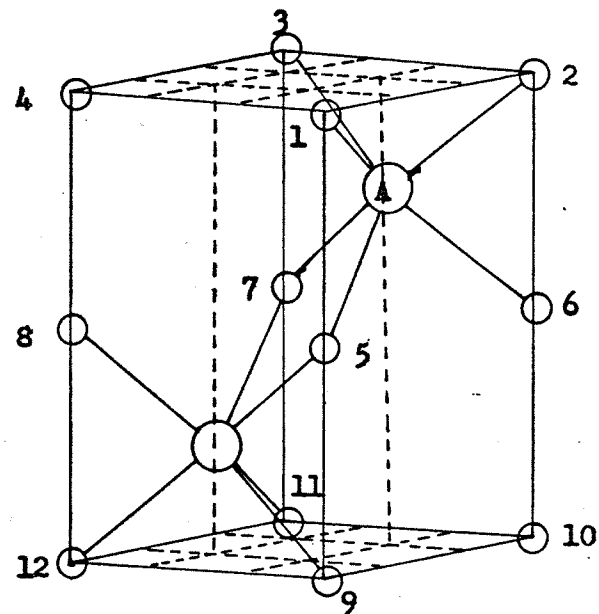
(a)



○ metal atom (e.g. Ni)

○ metalloid atom (e.g. As)

(b)



○ metal atom (e.g. Ni)

○ metalloid atom (e.g. As)

respectively. Thus the transition metal atoms occupy octahedral holes in the close-packed hexagonal array of metalloid atoms (e.g. referring to figure 1a, metal atom 1 is in the centre of the octahedron formed by metalloid atoms A, B, C, D, E, and F) and each metalloid atom is surrounded by six transition metal atoms in the form of a trigonal prism (e.g. referring to figure 1b, metalloid atom A is in the centre of the trigonal prism formed by metal atoms 1, 2, 3, 5, 6 and 7), the metalloid atoms forming alternate layers between metal atoms along the C-axis.

Figure 2 shows projections of the structure on the $y = 0$ and $z = 0$ planes of the unit cell and shows the lattice parameters, a and c . For ideal close-packing, the lattice parameter ratio, c/a , is 1.633.

The NiAs unit cell thus contains two metal atoms and two metalloid atoms giving the stoichiometric formula MX , where M represents the metal and the X the metalloid.

One of the main features of the nickel arsenide structure is its ability to take up transition metal atoms in the two trigonal prismatic holes formed by metal atoms 5, 6, 7, 9, 10, 11 and 1, 3, 4, 5, 7, 8 in figure 1b. When both of these holes are filled there are four metal atoms and two metalloid atoms per unit cell so that the structure corresponds to the stoichiometric composition M_2X and is referred to as the "filled up" or Ni_2In type shown in

FIGURE 2

THE NICKEL ARSENIDE STRUCTURE

Projections on the $y = 0$ and $z = 0$ planes.

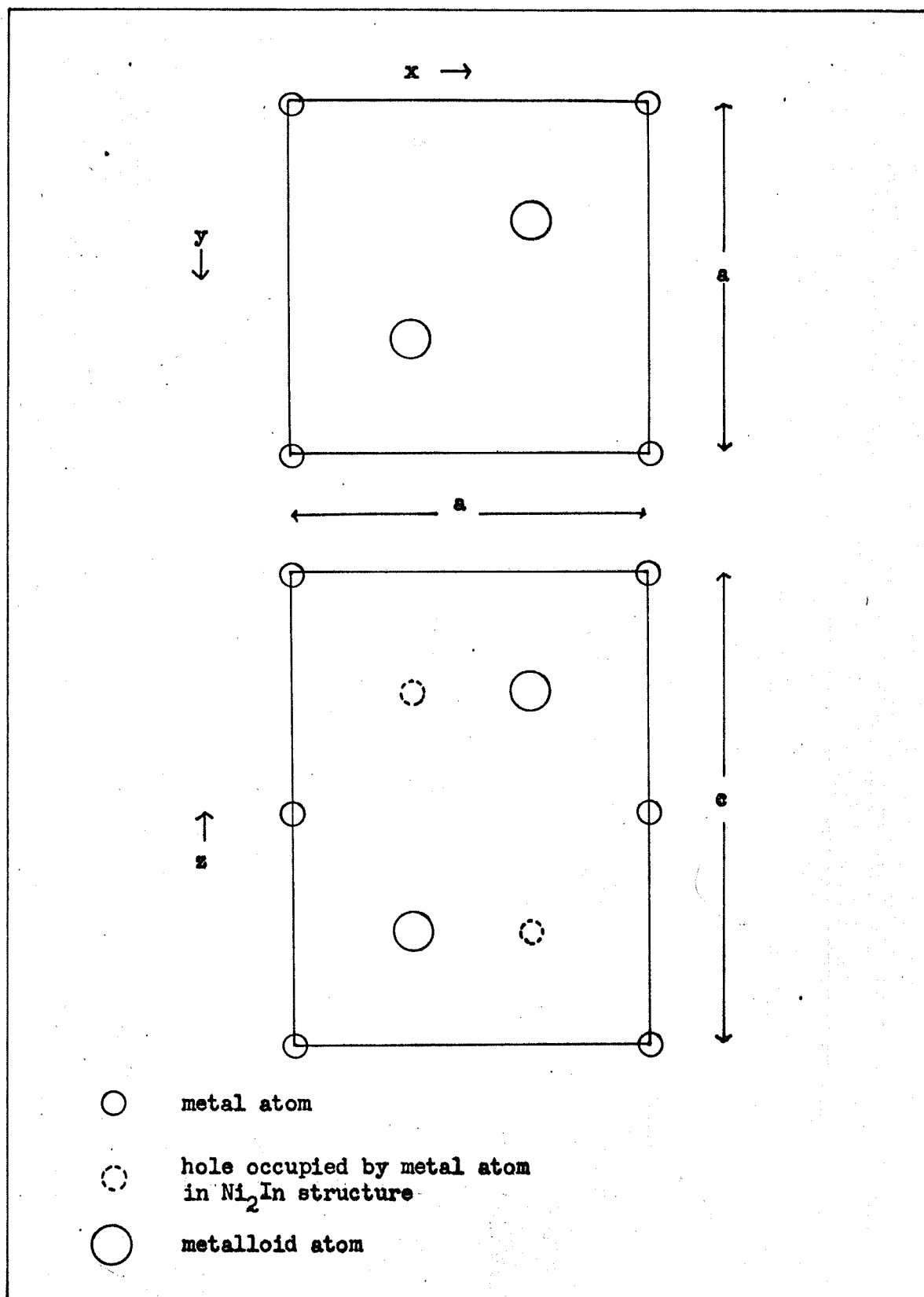


figure 3a. The structure can also omit transition metal atoms from positions 5, 6, 7 and 8 of figure 1b. When all four of these sites are vacant the unit cell contains one metal atom and two metalloid atoms giving the formula MX_2 . At this limit, alternate planes of transition metal atoms in the $[001]$ direction are missing and the structure is of the trigonal $Cd(OH)_2$ type shown in figure 3b. Thus the term "NiAs-type" may be used to refer to the group of structures with compositions from M_2X through MX to MX_2 , although the specific NiAs structure is that occurring at the composition MX .

It appears to be generally accepted that the low coefficients of friction observed for the diselenides of the transition metals are related to the layer-like $Cd(OH)_2$ structure they possess, in which metal atoms are absent between alternate layers of metalloid atoms, presumably weakening the bonding in the z-direction and permitting relatively free lateral movement between layers.

C. ESTABLISHED PHASES

The phases which have been identified in each of the metal-selenium systems of Ti, V, Cr, Zr, Nb, Mo, Hf, Ta, W and Re are listed in table 1. The purpose of including this information is primarily to aid in identifying the vaporization processes which were observed in this study. An attempt is made under the heading "DISCUSSION" to

FIGURE 3

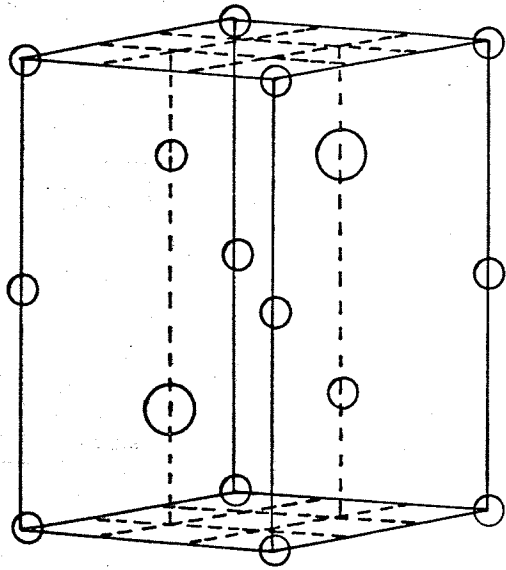
STRUCTURES RELATED TO THE NICKEL ARSENIDE TYPE

(a) The Ni_2In type

(b) The $\text{Cd}(\text{OH})_2$ type

○ metal atom

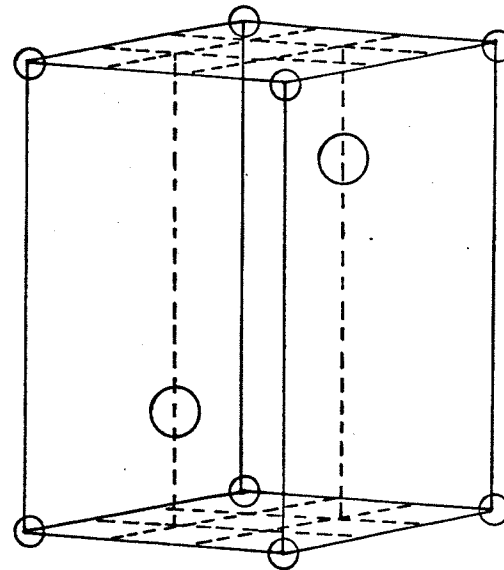
○ metalloloid atom



(a)

○ metal atom

○ metalloloid atom



(b)

relate the observed weight changes to transitions between the previously reported phases listed in table 1.

Where sufficient information is available, the entry for each phase includes the range of composition over which it is stable, the temperature at which it was prepared, its structure type and its lattice parameters. For some phases, the only information which could be found was that such compositions had been prepared by the cited authors. The formulae used in column one to designate the phases and the stability ranges listed in column two are those which are given by the authors referred to in column nine. In those cases where the original reference did not specify a stability range, the atomic percentage of selenium was calculated from the quoted formula and is given in brackets.

The information in table 1 is summarized in figure 4 in which the phases in each of the metal-selenium systems are shown on one dimensional composition diagrams. The type of structure exhibited by each phase is indicated by the type of cross-hatching.

D. THERMAL PROPERTIES

In comparison with the crystallographic, electrical and magnetic data which have been published for these compounds, very little seems to be known about their thermal properties. The information which is available may be summarized thus: the selenides of the transition

TABLE 1

REPORTED PHASES IN SOME TRANSITION METAL-SELENIUM SYSTEMS

(a) The Ti-Se System

Designation	Stability Range (Atom % Se)	Preparation Temperature (° C)	Structure Type	Lattice Parameters				Reference
				a (Å)	b (Å)	c (Å)	c/a or β (°)	
Ti ₉ Se ₄	(30.8)	500 & 900	ortho.**	3.43	11.68	14.47	-	24
Ti ₃ Se ₂	33.3-40.0	800 - 1000	NiAs	3.577	-	6.309	1.764	25
TiSe _{0.95}	~ 48.72 only	600-800	MnP	6.222	3.494	6.462	-	26
TiSe	(50.0)	800 - 1000	super- structure	7.149	-	11.99	1.68	4,25
TiSe	(50.0)	800 - 1000	super- structure	7.202	-	27.41	3.81	25
TiSe _{1.05} *	~ 52.22	600-800	NiAs	3.571	-	6.301	1.764	26
Ti _{1-x} Se	52.2-54.5	800	hex.	3.572	-	6.205	1.737	9,10
TiSe _{1.20}	54.55-	600-800	NiAs	3.572	-	6.195	1.734	26
TiSe _{1.30}	-56.52-~58.3	600-800	Fe ₃ Se ₄ ?	6.378	3.564	12.024	90.92	26
Ti ₃ Se ₄	(57.1)	1100	monocl. NiAs	13.66	3.571	12.02	152.92	9,10, 27

Designation	Stability Range (Atom % Se)	Preparation Temperature (° C)	Structure Type	Lattice Parameters				Reference
				a (Å)	b (Å)	c (Å)	c/a or β (°)	
Ti ₃ Se ₄	~57.4 only	1000	monocl. NiAs	-	-	-	-	28
Ti ₂ Se ₃	60.1	800	Cd(OH) ₂	3.595	-	5.994	1.667	4
Ti ₅ Se ₈	(61.5)	1100	monocl.	3.608	6.19	11.94	90.33	9,10, 29
TiSe ₂	~58.3-66.67	600-800	Cd(OH) ₂	3.537	-	6.005	1.698	26
TiSe ₂	(66.7)	550-580	Cd(OH) ₂	3.535	-	6.004	1.698	4
TiSe ₂	(66.7)	450-550	Cd(OH) ₂	3.539	-	6.004	1.697	9,10

* It has been suggested⁽³⁾ that this is probably identical with the phase designated Ti₃Se₂.

** The following abbreviations have been used in this table:

ortho.	orthorhombic
hex.	hexagonal
monocl.	monoclinic
tetrag.	tetragonal
sym.	symmetry
amorph.	amorphous

(b) The V-Se System

Designation	Stability Range (Atom % Se)	Preparation Temperature (° C)	Structure Type	Lattice Parameters				Reference
				a (Å)	b (Å)	c (Å)	c/a or β (°)	
VSe	51.0-~53.5*	1000	NiAs	3.587	-	5.989	1.670	30
V ₂ Se ₃	55.5-61.5	-	Lower sym. than hex.	-	-	-	-	30
V ₃ Se ₄	(57.1)	-	monocl. NiAs	-	-	-	-	27
V ₅ Se ₈	(61.5)	-	monocl. NiAs	-	-	-	-	31
VSe ₂	62.0-~66.7	-	Cd(OH) ₂	3.355 ^{**}	-	6.134 ^{**}	1.828 ^{**}	30
VSe ₂	(66.7)	-	Cd(OH) ₂	3.410 ^{**}	-	5.989 ^{**}	1.756 ^{**}	30

* Between ~53.5 and ~62.0 atom % Se there are NiAs-like lower symmetry structures.

** At 66.3 atom % Se.

*** At 61.8 atom % Se.

(c) The Cr-Se System

Designation	Stability Range (Atom % Se)	Preparation Temperature (° C)	Structure Type	Lattice Parameters				Reference
				a (Å)	b (Å)	c (Å)	c/a or β (°)	
Cr _{1-x} Se	~ 50.0-53.5	900	NiAs	3.691 [*]	-	6.031 [*]	1.633 [*]	32
Cr ₇ Se ₈	(53.3)	1100	Cr ₇ Se ₈	12.67	7.37	11.98	90.95	33
Cr _{1-x} Se	54.1-58.3	900	Fe ₃ Se ₄ ?	6.309 ^{**}	3.609 ^{**}	5.864 ^{**}	91.50 ^{**}	32
Cr ₃ Se ₄	(57.1)	1100	Fe ₃ Se ₄	6.32	3.62	11.77	91.47	33,34
Cr _{1-x} Se	58.85-59.7	900	NiAs	3.611 ^{***}	-	5.781 ^{***}	1.601 ^{***}	32

* At 50.0 atom % Se

** At 57.1 atom % Se

*** At 59.7 atom % Se

(d) The Zr-Se System

Designation	Stability Range (Atom % Se)	Preparation Temperature (° C)	Structure Type	Lattice Parameters				Reference
				a (Å)	b (Å)	c (Å)	c/a or β (°)	
Zr ₃ Se ₂	37.5-44.4	-	WC	-	-	-	-	35
Zr ₄ Se ₃	(42.9)	-	tetrag.	-	-	-	-	35
ZrSe	(50.0)	Absorbs O ₂ rapidly in air. X-ray data showed a mixture of Zr and ZrSe ₂ .						4
Zr ₃ Se ₄	50.0-58.3	-	distorted NaCl	-	-	-	-	35
Zr ₂ Se ₃	(60.0)	800	new type of hex.	3.757	-	18.63	4.959	4
ZrSe ₂	~63-66.7	800-900	Cd(OH) ₂	3.771	-	6.148	1.630	4,35
ZrSe ₃	(75.0)	600	monocl.	-	-	-	-	4,35

(e) The Nb-Se System

Designation	Stability Range (Atom % Se)	Preparation Temperature (° C)	Structure Type	Lattice Parameters				Reference
				a (Å)	b (Å)	c (Å)	c/a or β (°)	
Nb ₅ Se ₄	(44.4)	-	Tetrag. Ti ₅ Te ₄	9.871	-	3.4529	0.3498	36,37
NbSe	(50.0)	-	NiAs	-	-	-	-	38
Nb ₃ Se ₄	(57.1)	-	distorted Cd(OH) ₂	10.012	-	3.4707	0.3467	37,39
Nb _{1+x} Se ₂	60.8	-	NbS ₂ *	3.450	-	13.02	3.774	37,40
Nb _{1+x} Se ₂	61.5	Quenched from 1000	-	3.425	-	12.92	3.743	37,40
Nb _{1+x} Se ₂	66.7	-	-	3.446	-	12.55	3.643	37,40
NbSe ₂	65.6-66.7	600-800	NbS ₂ **	-	-	-	-	41
NbSe ₂	65.6-66.7	850-1000	NbS ₂ ** 4-layer	-	-	-	-	41
NbSe ₂	(66.7)	-	***	-	-	-	-	38,42
NbSe ₂	(66.7)	-	2, 3 and 4- layer NbS ₂	-	-	-	-	14

Designation	Stability Range (Atom % Se)	Preparation Temperature (° C)	Structure Type	Lattice Parameters				Reference
				a (Å)	b (Å)	c (Å)	c/a, or β (°)	
NbSe ₃	(75.0)	-	not layered	-	-	-	-	38
α NbSe ₄	(80.0)	-	Tetrag.	28.57	-	3.863	0.1343	43
β NbSe ₄	(80.0)	-	Tetrag.	9.503	-	19.15	2.015	43

* The NbS₂ structure is a 2-layer Cd(OH)₂ type.

** At room temperature, the 4-layer form transforms to the 2-layer form.

*** A layer structure in which the metal atoms have distorted octahedral or regular trigonal prismatic metalloid atom coordination.

(f) The Mo-Se System

Designation	Stability Range (Atom % Se)	Preparation Temperature (° C)	Structure Type	Lattice Parameters				Reference
				a (Å)	b (Å)	c (Å)	c/a or β (°)	
Mo ₂ Se ₃	(60.0)	-	-	-	-	-	-	18
MoSe ₂	(66.7)	-	MoS ₂ *	3.288	-	12.931	3.933	44,45
Mo ₂ Se ₅	(71.4)	-	-	-	-	-	-	18
MoSe ₃	(75.0)	-	amorph.	-	-	-	-	18
MoSe ₅	(83.3)	-	-	-	-	-	-	18

* The MoS₂ structure is a two layer Cd(OH)₂ type.

(g) The Hf-Se System

Designation	Stability Range (Atom % Se)	Preparation Temperature (° C)	Structure Type	Lattice Parameters				Reference
				a (Å)	b (Å)	c (Å)	c/a or β (°)	
HfSe	(50.0)	Takes up O ₂	rapidly from the air					4
Hf ₂ Se ₃	(60.0)	800	Complex diffraction pattern could not be indexed					4
HfSe ₂	(66.7)	900	Cd(OH) ₂	3.748	-	6.159	1.643	4
HfSe ₃	(75.0)	600	monocl.	-	-	-	-	4

(h) The Ta-Se System

Designation	Stability Range (Atom % Se)	Preparation Temperature (° C)	Structure Type	Lattice Parameters				Reference
				a (Å)	b (Å)	c (Å)	c/a or β (°)	
TaSe	(50.0)	-	-	-	-	-	-	38
Ta _{1+x} Se ₂	55.0-66.7	-	-	-	-	-	-	37
β TaSe _{1.98}	66.4	850 + slow cooling	lamellar hex.	3.429	-	12.73	3.712	46
δ TaSe _{1.98}	66.4	900-1100	lamellar hex.	3.46	-	37.9	10.95	46
TaSe ₂	(66.7)	750	Cd(OH) ₂	3.44	-	6.27	1.82	46
TaSe ₂	(66.7)	-	*	-	-	-	-	14
TaSe ₃	(75.0)	-	monocl.	10.402	3.495	9.829	106.26	47,48
TaSe ₃	(75.0)	750	monocl.	10.00	3.50	9.48	91.60	49

* 2, 3, 4 and 6-layer Cd(OH)₂ related types were reported.

(i) The W-Se System

Designation	Stability Range (Atom % Se)	Preparation Temperature (° C)	Structure Type	Lattice Parameters				Reference
				a (Å)	b (Å)	c (Å)	c/a or β (°)	
WSe ₂	66.1-66.7	-	MoS ₂	3.29	-	12.97	3.94	50,51
WSe ₃	(75.0)	-	amorph.	-	-	-	-	51

(j) The Re-Se System

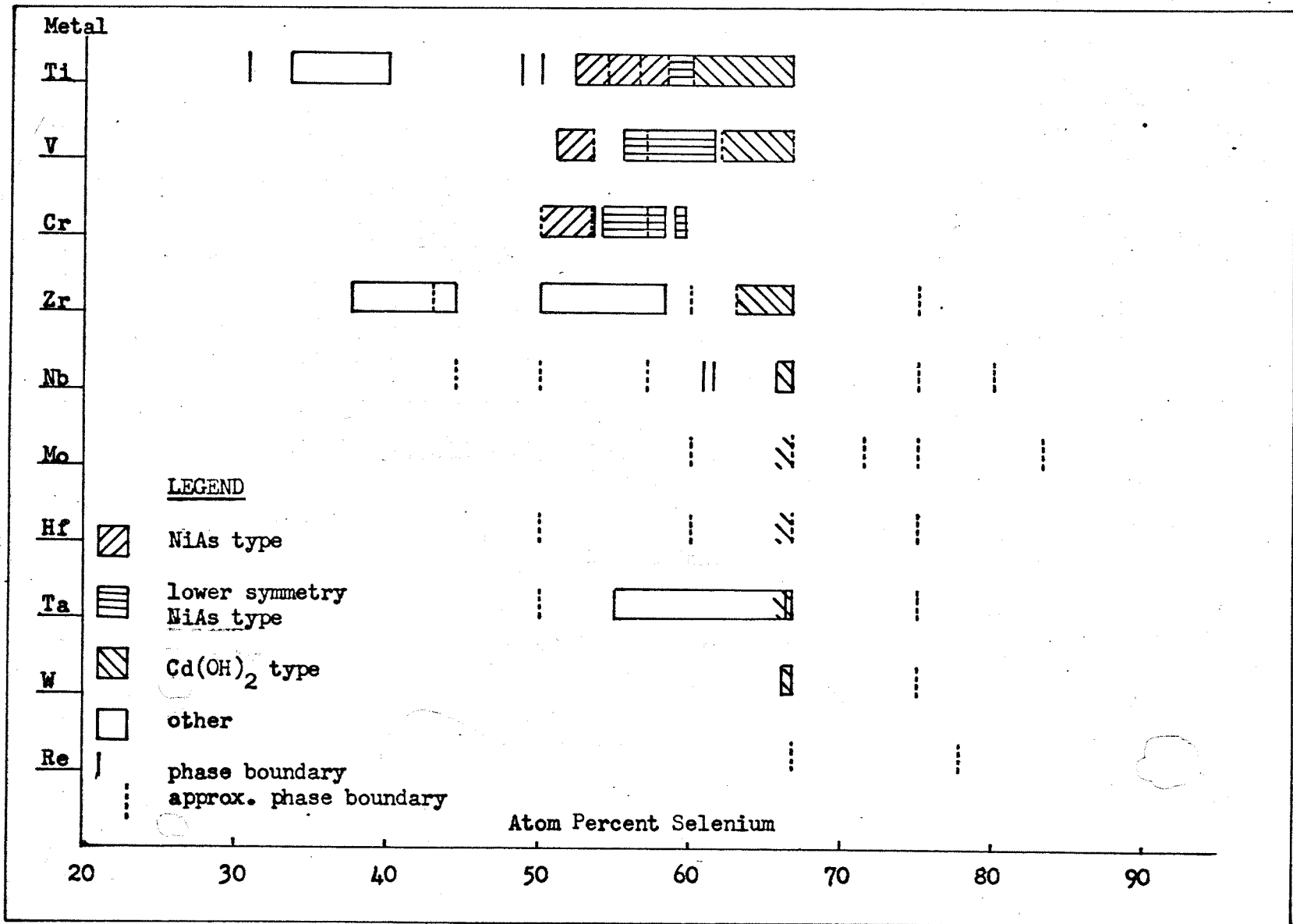
Designation	Stability Range (Atom % Se)	Preparation Temperature (° C)	Structure Type	Lattice Parameters				Reference
				a (Å)	b (Å)	c (Å)	c/a or β (°)	
ReSe ₂	(66.7)	-	Triclinic	6.727	6.603	6.720*	-	52
Re ₂ Se ₇	(77.8)	-	-	-	-	-	-	53

* $\alpha=118.94$ $\beta=91.83$ $\gamma=104.93$

FIGURE 4

TRANSITION METAL-SELENIUM SYSTEMS

One dimensional composition diagrams

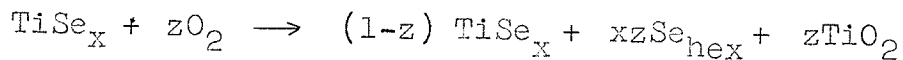


metals are, in general, quite stable in vacuum to several hundred degrees centigrade, after which they tend to lose selenium to form lower selenides, the decomposition sometimes going as far as the pure metal, while in air they all combine with oxygen to at least a small extent at room temperature and most oxidize quite rapidly at a few hundred degrees centigrade.

The available information on the thermal stability of the selenides of the group IVb, Vb, and VIb transition metals is detailed below.

(a) The Ti-Se System

Bear and McTaggart⁽⁷⁾ found that when TiSe_2 was heated in vacuum at 950°C it was degraded to $\text{TiSe}_{1.7}$. He pointed out that no phase change is involved in this process since the region $\text{TiSe}_{1.0}$ to $\text{TiSe}_{2.0}$ may be regarded as a single phase. The TiSe_2 used in his experiment had been prepared directly from the elements and excess selenium had been sublimed away by heating the product in vacuum at 450°C . Presumably it was felt that no decomposition occurred at that temperature. The same authors found that TiSe_2 heated in highly purified hydrogen at 950°C for three hours was reduced to $\text{TiSe}_{1.4}$. Bernusset⁽¹⁰⁾ found that the phases TiSe_2 , Ti_5Se_8 , Ti_3Se_4 and $\text{TiSe}_{1.09-1.20}$ are unstable in air and proposed that the reaction is:



He also reported⁽⁹⁾ that, for analysis the compounds may be sintered in air at 950° C when they form SeO₂ gas and TiO₂. The TiO₂ is then weighed to determine the titanium content of the original selenide.

Bear and McTaggart⁽⁷⁾ found that 15% of a sample of TiSe₂ oxidized when the sample was heated in air at 150° C for 10 days and 70% oxidized at 300° C in 3 days.

(b) The Cr-Se System

In 1880 in the first report of Cr₂Se₃⁽¹⁹⁾, Moissan states that the compound forms CrSe when heated out of contact with air.

(c) The Zr-Se System

Bear and McTaggart⁽⁷⁾ found that ZrSe₃ prepared by direct synthesis from the elements and freed from excess selenium by heating in vacuum to 450° C was analyzed to be ZrSe_{2.9}. This product when heated at 950° C in vacuum was degraded to ZrSe_{1.9}. They also found that hydrogen reduction of ZrSe₂ at 950° C for 3 hours gave ZrSe_{1.7}.

McTaggart and Wadsley⁽⁴⁾ found that ZrSe absorbs oxygen from the air too rapidly for them to perform accurate density or X-ray measurements. Bear and McTaggart⁽⁷⁾ measured the oxidation rate of ZrSe₃, ZrSe₂

and ZrSe in air at 150° C and 300° C. Their results are shown in table 2.

TABLE 2

OXIDATION OF Zr SELENIDES IN AIR

Compound	% of sample oxidized at:		
	150° C for 10 days	300° C for 1 day	300° C for 3 days
ZrSe ₃	20	35	70
ZrSe ₂	25	25	70
ZrSe	25	100	100

(d) The Mo-Se System

Taimni and Rakshpal⁽⁵⁴⁾ performed thermogravimetric analysis in vacuum on molybdenum selenide using a Stanton thermobalance. At a heating rate of 5.3 - 0.2° C per minute they found a horizontal level at 555 to 790° C which corresponded to the weight of the metal.

(e) The Hf-Se System

Bear and McTaggart⁽⁷⁾ prepared HfSe₃ by direct synthesis from the elements and removed excess selenium by subliming it away in vacuum at 450° C. The resulting product which was analyzed to be HfSe_{2.9}, was heated in vacuum at 940° C and found to give a degradation product

of $\text{HfSe}_{1.85}$. These authors also found that reduction of HfSe_2 in hydrogen at 940°C for 3 hours gave $\text{HfSe}_{1.75}$ as a product.

McTaggart and Wadsley⁽⁴⁾ reported that HfSe takes up oxygen from the air too rapidly to permit them to make accurate density or X-ray measurements.

(f) The Ta-Se System

Ariya, Zaslavsky and Matveeva⁽⁵⁰⁾ performed a thermogravimetric analysis on a sample with the composition $\text{TaSe}_{2.07}$. They heated the sample in vacuum increasing the temperature stepwise so that it was heated for 4 hours at each of 14 temperatures between 300°C and 900°C . The results show breaks in a plot of x versus temperature, where x is the number of selenium atoms per atom of tantalum, at $x = 2.06$, $T = 300^\circ \text{C}$; $x = 2.02$, $T = 560^\circ \text{C}$; $x = 2.00$, $T = 850^\circ \text{C}$ and $x = 1.98$, $T = 900^\circ \text{C}$. Above 900°C decomposition of the selenide becomes rapid.

Aslanov, Simanov, Novoselova and Ukrainskii⁽⁴⁹⁾ report that TaSe_3 decomposes in vacuum to TaSe_2 and Se at $780 - 785^\circ \text{C}$. Bjerkelund⁽⁴⁷⁾ on the other hand found that TaSe_3 began to decompose at 160°C when he recorded a gradual fall in resistivity with time at constant temperature.

(g) The W-Se System

Uelsmann⁽¹⁷⁾, in an early report of the preparation of WSe_3 noted that when the compound is heated out of contact with air it forms WSe_2 and selenium.

(h) The Re-Se System

Briscoe, Robinson and Stoddart⁽⁵³⁾ found that Re_2Se_7 undergoes thermal decomposition in vacuum at 325 to 330° C to form $ReSe_2$.

No thermal information could be found for either the V-Se or Nb-Se systems.

PART THREE: PRINCIPLES OF THERMOGRAVIMETRIC ANALYSIS

A. QUALITATIVE ANALYSIS

1. Information Obtainable from Weight Versus Time and Weight Versus Temperature Measurements.

Thermogravimetric analysis (T.G.A.) may be defined as the continuous measurement of the weight of a sample as its temperature is controlled. There are two common types of T.G.A. experiments. The sample weight may be recorded as the temperature is increased at a controlled rate, or it may be measured as a function of time while the temperature is kept constant. During the experiment, the sample may be in an inert or reactive atmosphere or in a vacuum.

T.G.A. in which the temperature is continuously increased provides a method by which a large temperature range may be surveyed for initiation temperatures of reactions such as oxidations and decompositions, which involve weight changes. The magnitude of any weight change observed can be of considerable help in identifying the reaction which is occurring. This type of experiment is often used as a method of qualitative analysis.

Constant temperature T.G.A. may also be used to obtain qualitative information. In general, different processes occur at different rates at the same temperature, so that a graph of weight as a function of time will show a change of slope as one process ends and another begins.

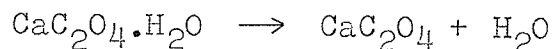
2. Limitations of Qualitative T.G.A.

Thermogravimetric analysis suffers from a number of inherent limitations which are important to consider in the planning and interpretation of T.G.A. experiments. Garn⁽⁵⁵⁾ has discussed these limitations in some detail. If the weighing is performed in vacuum, so that changes in bouyancy of the atmosphere and movement of gases by convection are negligible, the principle problem in qualitative applications of T.G.A. is that associated with heat transfer and the consequent temperature lag.

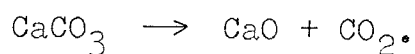
In order to raise the temperature of a sample, heat must be transferred to it from a furnace of some type. This implies a temperature difference between the furnace and the sample and therefore a temperature measurement anywhere but in the sample will be in error. The higher the heating rate the more the sample temperature will lag behind that of the furnace. The error is aggravated in T.G.A. because, in order to weigh the sample with adequate accuracy and sensitivity, mechanical contact with it must be extremely light. Thus, the temperature difference cannot be reduced by placing the sample in direct contact with the furnace nor, as is common practice in differential thermal analysis by mounting the sample in a block of high conductivity material. Unfortunately the temperature lag is often changed at the temperature of most interest, i.e.

at the reaction temperature because for most reactions heat is either absorbed or released by the sample.

The magnitude of these effects has been measured by Newkirk⁽⁵⁶⁾ in a study of the sources of error in a Chevenard thermobalance. He measured at several temperatures the difference in temperature between a control thermocouple in the furnace and another thermocouple in the sample holder. Figure 5a shows the effect of heating rate on the temperature lag of an empty sample holder. At a heating rate of 2.5° C per minute the maximum lag is approximately 7° C while at 10° C per minute it is approximately 14° C. The lag increases with temperature at first, then becomes more constant as heat transfer processes become more effective at higher temperatures. Fortunately, low heating rates are commonly used in T.G.A. Figure 5b shows how the temperature lag may be affected by the presence of a sample. At a heating rate of 10° C per minute, the presence of 600 mg. of $\text{CaC}_2\text{O}_4 \cdot \text{H}_2\text{O}$ causes the lag to more than double at the temperatures of the decompositions:



and subsequently:



Between these reactions the decomposition:

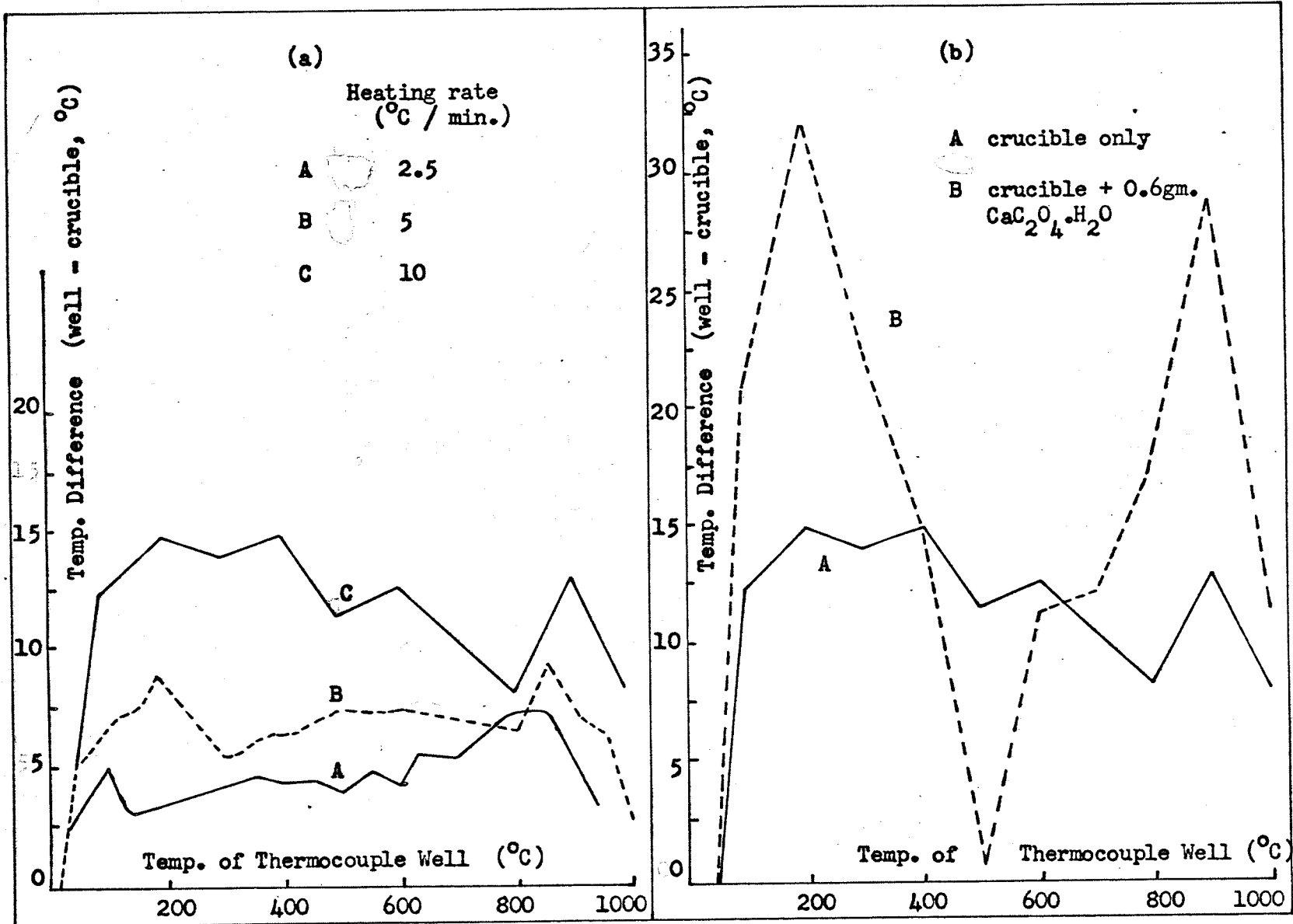
FIGURE 5

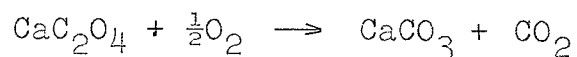
TEMPERATURE ERRORS IN A CHEVENARD THERMOBALANCE

Temperature lag of sample holder
with respect to furnace temperature

- (a) Effect of heating rate
- (b) Effect of sample

From Newkirk⁽⁵⁶⁾





gives off enough heat to bring the crucible very near the furnace temperature. It should be noted that, as in many thermobalances, the Chevenard balance which Newkirk used for this study has a very light sample holder, so that the sample contributes most of the heat capacity.

In the type of T.G.A. experiment in which the temperature is continuously changed, it appears that temperature equilibrium is unlikely to be attained, therefore temperatures of reaction obtained from such experiments may not be reliable. In constant temperature measurements, the problem should not be as serious. If the temperature is high enough for heat transfer to the sample to be reasonably efficient, if the sample is small so that its heat capacity is small compared with the sample holder and if the heat absorbed or evolved by the sample during the reaction is small, then it may be reasonable to assume that the sample temperature is constant and equal to that indicated by a thermocouple placed between the sample and the furnace.

B. VAPOR PRESSURE MEASUREMENT

1. Evaporation Theory

Under certain conditions, T.G.A. may be used to obtain quantitative information about the processes

occurring in a sample as it is heated. In particular, the experiment may be made to conform to either Langmuir's or Knudsen's method for measuring vapor pressure. In these methods, the net vaporization rate of a sample is obtained by measuring its rate of weight loss at constant temperature. It is possible to derive equations relating these rates of vaporization to vapor pressure. The equations are based on a "direct evaporation theory" and the kinetic theory of gases.

The term "direct evaporation theory" is used to distinguish it from the more detailed theories which are required to explain microscopic observations of the process of vaporization. There are two assumptions basic to the direct evaporation theory. The first is that every vapour molecule which strikes the surface of the solid will condense onto it i.e. will be "captured". The second is that every molecule in the surface layer of the solid is bound there by an energy equivalent to the latent heat of sublimation per molecule, so that as soon as it attains that energy it will transfer directly into the vapor phase. This model implies that for a given substance the probability of being transferred into the vapor phase is the same for every particle in the surface and depends only on the temperature, and that the rate of condensation depends only on the vapor pressure above the solid. Furthermore, the

processes of evaporation and condensation are considered not to interact with each other so that, for instance, the rate of evaporation is not significantly affected by the presence or absence of a vapor phase above the solid surface. The relative magnitudes of the two independent rates determines whether there is equilibrium or a resultant vaporization or condensation.

2. Langmuir's Method of Vapor Pressure Measurement

This method was published by the German physicist I. Langmuir in 1913⁽⁵⁷⁾. It is a non-equilibrium method in which the sample is allowed to freely evaporate into a vacuum and the weight loss per unit area is measured as a function of time at constant temperature. The vapor pressure of the sample may be calculated from this net vaporization rate in the following way:

From the kinetic theory of gases it may be shown that the number of molecules of a vapor which strike a surface area $A \text{ cm}^2$ in unit time is given by:

$$\begin{aligned} G &= AP \left[2\pi mkT \right]^{-\frac{1}{2}} \text{ molecules sec.}^{-1} \text{ - - - - - } 1 \\ &= AP \left[2\pi MRT \right]^{-\frac{1}{2}} \text{ moles. sec.}^{-1} \\ &= AP \left[\frac{M}{2\pi RT} \right]^{\frac{1}{2}} \text{ gm. sec.}^{-1} \end{aligned}$$

where P = pressure of the vapor above the surface

$$(\text{dyne cm}^{-2})$$

m = mass of one molecule of vapor

$$(\text{gm. molecule}^{-1})$$

k = the Boltzmann constant

$$(\text{erg deg.}^{-1} \text{ mol.}^{-1})$$

T = temperature of the surface

$$(\text{deg.})$$

M = molecular weight of the vapor

$$(\text{gm. mole}^{-1})$$

R = the gas constant

$$(\text{=Nk=gm. cm.}^2 \text{ sec.}^{-2} \text{ deg.}^{-1} \text{ mole}^{-1})$$

The basic assumption that every vapor molecule striking the solid surface is captured means that the rate of condensation, G_c , is given by equations (1) with A being the surface area of the sample. Under equilibrium conditions, the pressure, P , of the vapor above the solid surface is the saturated or equilibrium vapor pressure, P_e , of the substance, so that:

$$G_c = AP_e [2\pi MRT]^{-\frac{1}{2}} \text{ moles sec.}^{-1} \text{ - - - - 2}$$

However, at equilibrium, the rate of condensation is equal to the rate of vaporization, G_v , therefore:

$$G_v = AP_e [2\pi MRT]^{-\frac{1}{2}} \text{ moles sec.}^{-1} \text{ - - - - 3}$$

Equation (3) is the Langmuir-Knudsen equation for evaporation into a vacuum. For any experimental conditions

intermediate between evaporation at equilibrium and into a vacuum, the net vaporization rate, G_{nv} , is given by:

$$G_{nv} = G_v - G_c = A (P_e - P) [2\pi MRT]^{-\frac{1}{2}} \text{ moles sec.}^{-1} \quad 4$$

where P is the pressure of the vapor above the surface and $0 < P \leq P_e$.

3. Knudsen's Method of Vapor Pressure Measurement.

The physicist M. Knudsen published this method of vapor pressure measurement in 1909⁽⁵⁷⁾. The vaporization rate is measured under conditions which are close to equilibrium by enclosing the sample in an effusion cell so that the vapor may escape only through a small orifice. The rate of effusion of vapor through the orifice is related to the vapor pressure of the sample by an argument similar to that used for Langmuir's method. As before, the rate of evaporation from the surface of the sample is given by equation (3). However, in an effusion cell, the steady state condition is that the rate of evaporation from the sample surface is equal to the sum of the rate of loss of vapor from the cell and the rate of condensation of vapor onto the solid surface. If the steady state pressure of the vapor in the cell is P , then the rate of condensation is:

$$G_c = AP [2\pi MRT]^{-\frac{1}{2}} \text{ moles sec.}^{-1} \quad \text{--- 5}$$

from Equation (1). Equation (1) may also be used to show that the rate of effusion, G_{eff} , of vapor through an orifice of area $a \text{ cm}^2$ is:

$$G_{\text{eff}} = a(P - P_0) [2\pi MRT]^{-\frac{1}{2}} \text{ moles sec.}^{-1} \text{ --- 6}$$

where P and P_0 are the pressures on the inside and outside of the orifice respectively. The steady state condition:

$$G_v = G_c + G_{\text{eff}} \text{ --- --- --- 7}$$

therefore may be written:

$$AP_e [2\pi MRT]^{-\frac{1}{2}} = AP [2\pi MRT]^{-\frac{1}{2}} + a(P - P_0) [2\pi MRT]^{-\frac{1}{2}}$$

$$\therefore P = \frac{AP_e - aP_0}{(A + a)} \text{ --- --- --- 8}$$

From equation (8) it is evident that, if $P_0 \ll P_e$ and $a \ll A$, then:

$$P \cong P_e \text{ --- --- --- 9}$$

Under these conditions, the measured rate of effusion is related to the equilibrium vapor pressure of the sample by:

$$G_{\text{eff}} = aP_e [2\pi MRT]^{-\frac{1}{2}} \text{ --- --- --- 10}$$

4. Uncertainties in Vapor Pressure Measurements

It is generally recognized⁽⁵⁷⁾ that measured rates of vaporization are often much lower than predicted by the simple theory of direct evaporation. In order to quantitatively characterize these discrepancies Knudsen (1909-1915)

inserted a coefficient, α , into the ideal Knudsen-Langmuir equation (equation (3)), so that it becomes:

$$G = \alpha P [2\pi MRT]^{-\frac{1}{2}} \text{ moles cm.}^{-2} \text{ sec.}^{-1}$$

The coefficient, α , has been variously called the vaporization coefficient, the evaporation coefficient and the accommodation coefficient. However, it has been defined, more or less consistently, as the ratio of the evaporation rate measured experimentally to the rate calculated by using the equilibrium vapor pressure in the ideal Langmuir-Knudsen equation. Thus α is a fraction ≤ 1 which permits a quantitative measure of the extent to which a substance deviates from the direct evaporation theory.

However, this definition includes deviations arising from purely experimental uncertainties as well as errors in the vaporization theory itself. In addition, many of the early vaporization studies were concerned with metals for which α is close to unity, so that little physical significance was attached to α at first. As details of the processes of evaporation and condensation became better understood, a more precise definition of the accommodation coefficient became possible. Hirth and Pound⁽⁵⁸⁾ point out that the coefficient multiplying the ideal Langmuir-Knudsen equation is in general different depending on whether net vaporization or condensation is

occurring. They therefore define two coefficients, α_v and α_c , the general evaporation coefficient and the general condensation coefficient respectively. The definitions are in terms of the net vaporization and condensation flux, G_{nv} and G_{nc} respectively as given by equation (4):

$$G_{nv} = \alpha_v (P_e - P) [2\pi MRT]^{-\frac{1}{2}} \text{ where } P_e > P \text{ and}$$

$$G_{nc} = \alpha_c (P - P_e) [2\pi MRT]^{-\frac{1}{2}} \text{ where } P > P_e$$

These workers further note that, according to more detailed evaporation theories, such as those of Knacke and Stranski⁽⁵⁹⁾, there may be several factors which contribute to making α_c or α_v less than unity. For each specific factor they define a specific condensation or evaporation coefficient. Thus the general coefficients are in general products of several specific coefficients i.e.:

$$\alpha_c = \prod_i \alpha_{c_i} \text{ and } \alpha_v = \prod_i \alpha_{v_i}$$

The Knacke and Stranski theory explains qualitatively many microscopic phenomena observed during vaporization and condensation, however it is unable as yet to calculate the condensation and evaporation coefficients for real substances and therefore cannot yet be of direct help in calculating vapor pressures from vaporization rates. The theory will therefore not be considered here in any further detail.

Until the theory reaches a more quantitative stage of development, these molecular factors must be considered as properties of the material being studied.

Even if it is assumed that the direct vaporization theory accurately describes the molecular processes occurring during the vaporization of a solid, there are several other factors which may affect the measured vaporization rate and thus contribute to an accommodation coefficient other than unity. These larger scale factors are in some cases amenable to some degree of experimental control, and therefore will be discussed further.

The vaporization rate is greatly affected by the state of sub-division of the sample. In order to calculate the vapor pressure from the Langmuir-Knudsen equation, it is necessary to know the surface area of the sample. An accurate measurement of this variable can be approached only in the case of single crystals. The surface area of polycrystalline or powdered samples is very difficult to determine. Even if this were possible, polycrystalline samples have other properties which cause difficulties. The inner channels and crevices of the powder may act as small Knudsen cells in which the evaporating molecule undergoes many collisions before leaving the solid, thereby establishing some degree of equilibrium between the solid and the vapor. The fraction of the surface where the vapor

pressure approaches the equilibrium value is indeterminate unless the vaporization is performed in a Knudsen cell. The surface area is more likely to change during the evaporation of a polycrystalline sample than during a single crystalline experiment, so that the vaporization rate is likely to be time dependent. Finally, due to the poor thermal conductivity of polycrystalline powders compared with single crystals, there is more likely to be a steep temperature gradient between the thermocouple and the surface of the sample.

The derivation of the equation relating the rate of effusion from a Knudsen cell to vapor pressure (equation (10)) assumes the absence of molecular collisions within the cell and in the orifice, i.e., conditions such that the mean free path for vapor molecules is at least an order of magnitude larger than the dimensions of the cell. In practice, this means that the equilibrium vapor pressure should be less than 10^{-1} mm. Hg. This requirement also means that the use of the ideal gas law in deriving the initial kinetic molecular theory equation (equation (1)) is justified.

In Knudsen experiments, the geometry of the cell should be such that:

(a) The ratio of length to diameter is less than 0.01 to ensure that resistance caused by the chamber walls

to molecular flow is negligible.

(b) The diaphragm containing the orifice is as thin as possible. For any appreciable thickness, effusion must be considered as taking place through a short pipe rather than an orifice. Clausing⁽⁶⁰⁾ has suggested a correction factor which allows for the resistance of the pipe to molecular flow. The Clausing factor (K) is given by the following expressions⁽⁵⁷⁾, depending on the ratio of the length of the orifice (L) to its radius (r):

$$\text{for } L/r \leq 1.5, K = \frac{1}{1 + 0.5 L/r}$$

$$\text{for } L/r > 1.5, K = \frac{1 + 0.4 L/r}{1 + 0.95 L/r + 0.15 (L/r)^2}$$

(c) The temperature is uniform over the entire volume of the cell. Special care should be taken to avoid overheating or underheating the diaphragm since the effusion rate is very sensitive to its temperature.

(d) The relative dimensions of the cell and orifice are such that the vapor in the cell can remain effectively saturated.

The cell material should be selected carefully. It should be inert towards the sample material, whether in solid or vapor form, and its vapor pressure at the temperature of the experiment should be several orders of magnitude smaller than that of the sample.

Self cooling of the surface during the evaporation of a solid is probably not an important source of error. Assuming approximate values for the emissivity of a solid sample and from its known heat of vaporization, Knacke and Stranski⁽⁵⁹⁾ have calculated the heat input and heat loss in single crystal experiments and have concluded that heat loss due to surface cooling is negligible.

Finally, it should be noted that equations (4) and (10) show that, in order to calculate vapor pressures from either Knudsen or Langmuir experiments, the molecular weight of the vapor must be known. Since the process of evaporation may be accompanied by molecular association or dissociation, it cannot be assumed that the gas phase will necessarily have the same molecular composition as the solid phase. The molecular weight of the vapor can be positively determined only by experiment.

APPARATUS AND PROCEDURE

PART FOUR: INTRODUCTION

The principle experimental technique used in this study was thermogravimetric analysis (T.G.A.). The apparatus with which the T.G.A. experiments were performed is described in part two of this chapter. The description includes details of the construction and operation of each component and reasons for some of the choices of design.

Part three contains details of the experiments for which the T.G.A. apparatus was used. It includes the procedure used to calibrate the thermobalance and a number of precautions which were found necessary to obtain reproducible results.

**PART FIVE: CONSTRUCTION AND OPERATION OF THE
THERMOGRAVIMETRIC APPARATUS**

A. GENERAL

The purpose of the apparatus is to permit the continuous automatic measurement of the weight and temperature of a sample as it is subjected to a controlled temperature and external pressure. Hence, the apparatus performs five functions: weight measurement, temperature control, temperature measurement, pressure control and pressure measurement. The components which accomplish each of these functions are described in detail below and are illustrated in figure 6.

B. WEIGHT MEASUREMENT

The sample is weighed on a top loading spring balance whose extension is continuously measured with a linear variable differential transformer (L.V.D.T.) and this weight measurement is recorded on a chart recorder. The main components of the weighing system are: the spring balance, the L.V.D.T. and the sample holder.

1. The Spring Balance

The components of the top loading spring balance are illustrated in figure 7. The sample is balanced above the spring by placing it on the top of a yoke to the bottom of which is attached a counterweight. The yoke is suspended from the bottom of the spring and the top of the spring is

FIGURE 6

THERMOGRAVIMETRIC APPARATUS
General Arrangement of Components

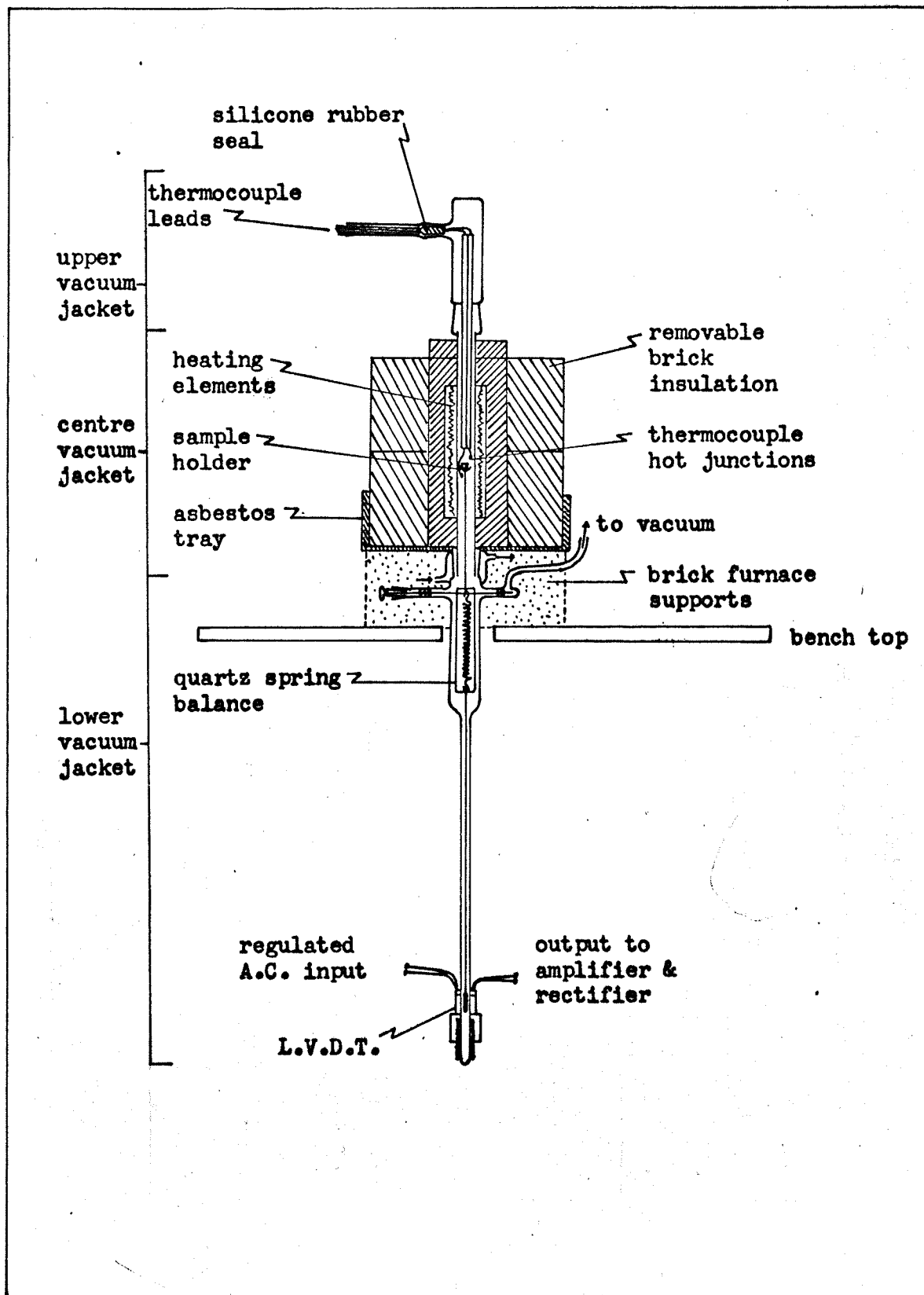
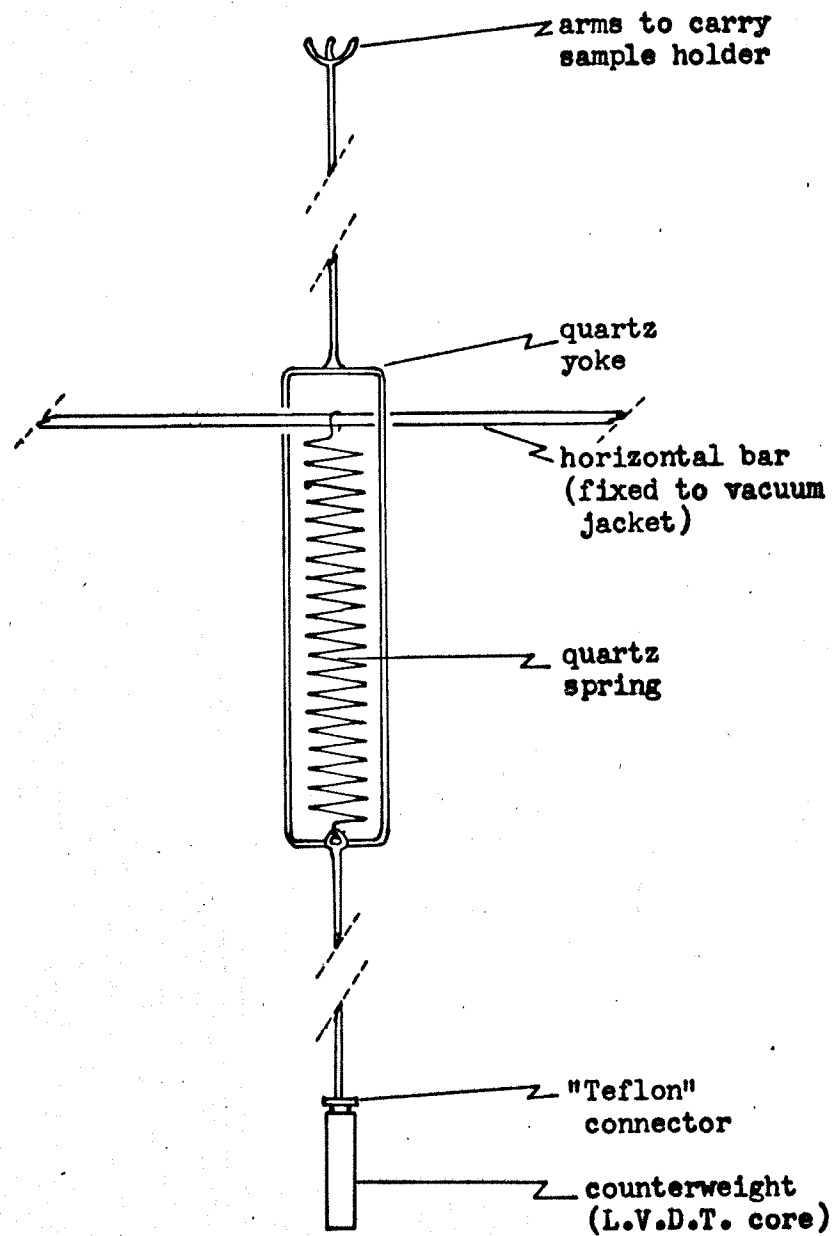


FIGURE 7

THERMOGRAVIMETRIC APPARATUS

The Spring Balance



hooked onto a fixed horizontal bar.

The spring is a quartz helix which was purchased from Worden Laboratories, 695 Rocky River, Houston, Texas. It has an extension of one centimeter per gram to a maximum load of ten grams.

The yoke is constructed of one millimeter diameter quartz rod and was made locally. Its top has three small arms formed so as to hold a cup-shaped sample holder.

The horizontal bar from which the spring is hung is a glass rod which passes through two plastic ("Teflon") spacers. The spacers fit into side arms in the lower vacuum jacket.

The core of the L.V.D.T. is used as the counter-weight. It is attached to the bottom of the yoke by a small "Teflon" connector which fits tightly over the lower end of the yoke and which screws into the core.

The original reason for using a top loading design was so that a sample could be lowered into place after the apparatus has reached equilibrium at a desired temperature. This arrangement would be advantageous when studying a fast reaction or the initial stages of a reaction at a constant temperature. Top loading has an additional advantage when operating under non-vacuum conditions. In a bottom loading system, the sample, and hence the furnace, is below the weight measuring mechanism. This arrangement

usually means that there is a cold zone above a hot zone, since most weighing mechanisms must be kept near room temperature. Under these conditions, convection currents may become a problem if the experiment is not performed under vacuum. With top loading, the hot and cold zones are in the correct order to minimize convection.

2. The L.V.D.T.

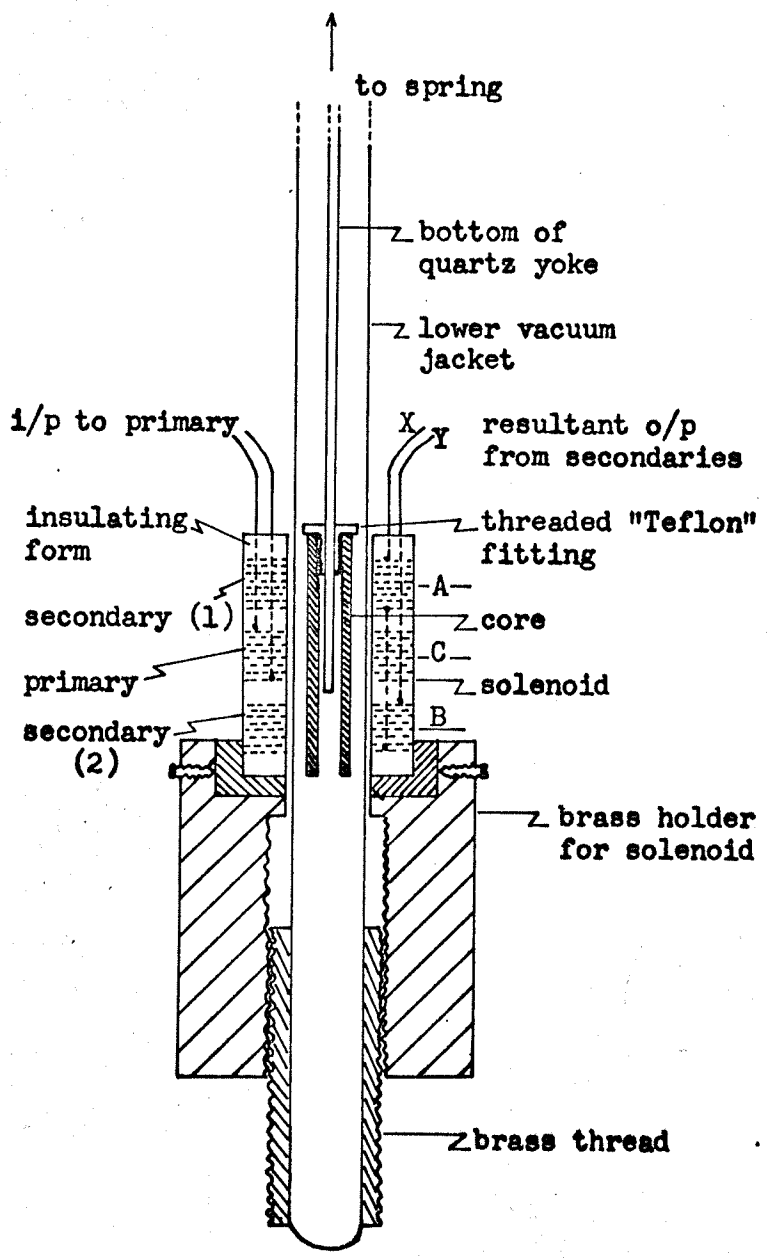
The degree of extension of the spring, and hence the weight of the sample, is measured with an L.V.D.T.. In order to clarify the description of this part of the apparatus, a brief account of the principles of operation of the L.V.D.T. will be presented.

An L.V.D.T. consists of a primary winding, two secondary windings and a movable core. The windings are arranged on a hollow, cylindrical, insulating form so that the primary is in the centre and there is one secondary at each end (see figure 8). When a constant A.C. voltage is applied to the primary winding, the current induced in each of the secondary windings is determined by the position of the core. The more the core couples the magnetic field produced by the primary current to a secondary, the greater will be the current induced in that secondary. When the centre of the core is at position A in figure 8, the current in secondary (1) is greater than in secondary (2), at position B, the current in (2) exceeds that in (1), and

FIGURE 8

THERMOGRAVIMETRIC APPARATUS

Cross Sectional View of the L.V.D.T. Assembly



at position C the two currents are equal. The windings of the two secondaries are connected together internally so that their A.C. currents are 180 degrees out of phase with respect to each other. At any instant, the resulting output at terminals (X,Y) is therefore the difference between the instantaneous currents in the two secondaries. As the core is moved from A to B, the resultant output first decreases in magnitude to zero at C, where the two currents exactly cancel each other, then increases again to B, but now with a phase 180 degrees different from the output at position A.

In the vicinity of position C, the null position, the L.V.D.T. output varies approximately linearly with the core position. Since the core of the L.V.D.T. is the counter-weight of the spring balance, the L.V.D.T. output indicates the degree of extension of the spring, and hence via Hooke's law, the weight of the sample.

The L.V.D.T. used in this apparatus is a type 175ES-L, serial number 0102, made by Schaevitz Engineering Co., P. O. Box 505, Camden 1, New Jersey. The core which was supplied with this L.V.D.T. has a diameter of $\frac{1}{4}$ inch. However, in order to provide sufficient clearance between the core and the inside of the vacuum jacket, a core of $\frac{3}{16}$ inch diameter is used.

In order to make adjustable the position of the L.V.D.T. solenoid relative to the core, the solenoid is

fitted to a hollow cylindrical brass holder. This holder may be screwed up and down a brass thread which is cemented with an epoxy adhesive to the outside of the base of the lower vacuum jacket. This arrangement, illustrated in figure 8, provides a finely adjustable and stable support for the transformer.

It was found essential to carefully regulate the input voltage to the L.V.D.T. primary. The most satisfactory results were obtained by using a properly loaded saturable-core constant-voltage transformer and a Zener diode. The circuit diagram is included in figure 9.

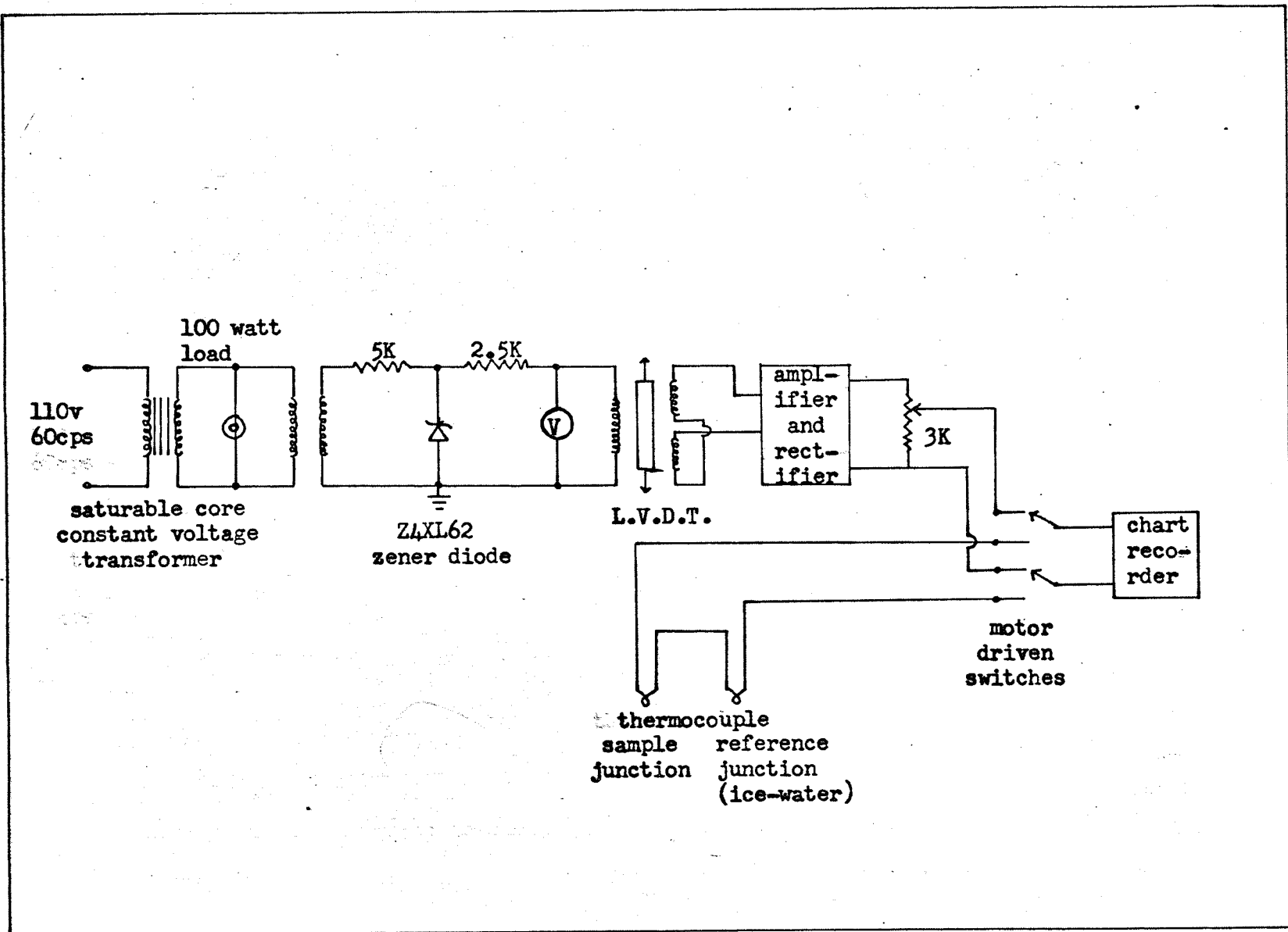
The input voltage provided to the L.V.D.T. primary is 0.3 volts r.m.s.. Although the L.V.D.T. may be used with a primary voltage as high as 6 volts, a lower value is used in order to minimize undesirable side effects which the magnetic field can have on the core. For example, the magnetic field will tend to pull the core towards the null position since the primary windings will tend to act as a solenoid⁽⁵⁵⁾. In addition it was found the core tends to be pulled towards the side of the transformer and at high input voltages the core touches the glass vacuum jacket and provides a serious source of friction in the balance system.

In order to record the L.V.D.T. output on a D.C. chart recorder, the A.C. voltage is first amplified and then rectified. The rectification step may be unnecessary, since

FIGURE 9

THERMOGRAVIMETRIC APPARATUS

Overall circuit diagram



the recorder converts the D.C. voltage back to A.C. with a chopper circuit in order to amplify it to drive the recorder servo system. It should be possible to bypass the rectifier and chopper circuits and insert the A.C. voltage from the L.V.D.T. directly into the recorder. Garn⁽⁵⁵⁾ has suggested that this could be conveniently accomplished by removing the chopper tube from the recorder and replacing it with a plug to fit the vacant socket. The plug could be suitably wired to correctly insert the L.V.D.T. output voltage into the recorder amplifiers previously supplied by the chopper.

However, this arrangement was not employed because considerable difficulty was encountered in obtaining a reliable recorder. When this was finally accomplished, it was considered better to allow the recorder to remain a separate, reliable component of the system.

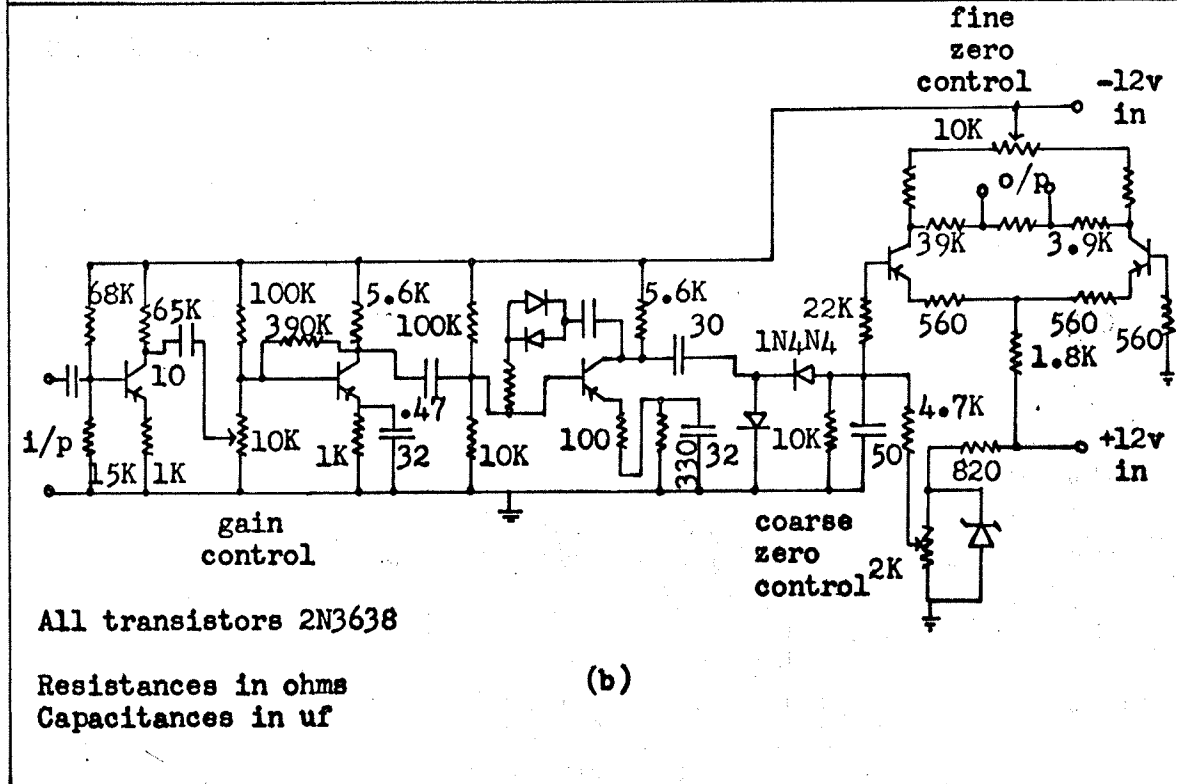
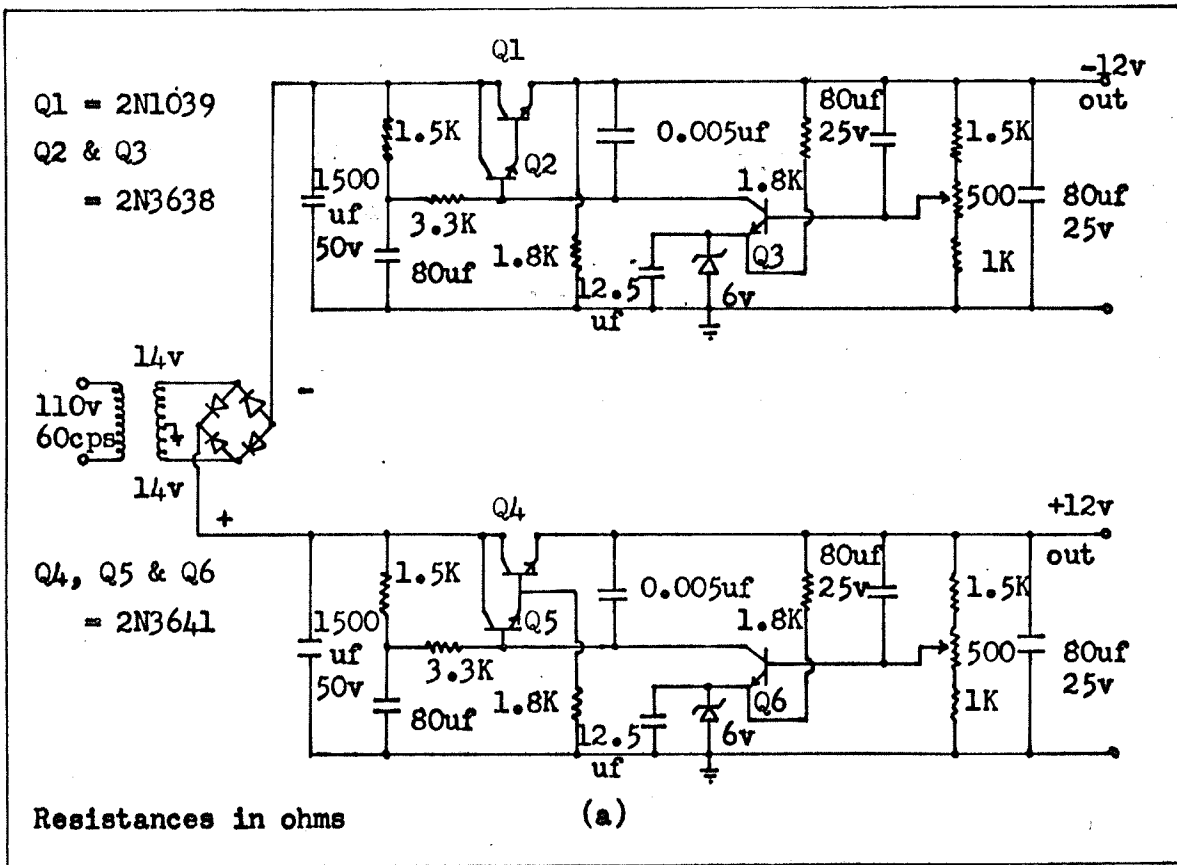
The amplifier-rectifier circuit is shown in figure 10. Incorporated into this circuit are a gain control and a zero shifting network. The zero shift is accomplished by adding to the rectifier output a positive or negative portion of a constant D.C. voltage supplied by a Zener diode. The gain control on the amplifier is a continuously adjustable potentiometer. In order to have reproducible gain settings, this control is set for maximum gain and the output is led to a 3 kilohm "Dekapot" decade resistance voltage divider (see figure 9) which permits accurately known and

FIGURE 10

THERMOGRAVIMETRIC APPARATUS

L.V.D.T. Amplifier-Rectifier Circuits

- (a) 12 volt power supply
- (b) 60 Hz amplifier and rectifier



reproducible fractions of the amplifier output to be fed to the recorder. The portion of the 3 kilohm resistance selected can be adjusted and read in one ohm steps with a continuously variable fine adjustment which can be read to ± 0.1 ohm and estimated to ± 0.01 ohm.

The outputs from the 3 kilohm voltage divider and from the thermocouple which measures the furnace temperature are recorded on the same chart recorder by means of a time sharing switching arrangement. The circuit is shown as part of figure 9. Cams driven by a 1/10 r.p.m. motor actuate two micro-switches which switch the recorder input from the L.V.D.T. to the thermocouple voltage and back again. The cams are adjustable, so that one input may be recorded for any desired portion of the 10 minute cycle of the motor, with the other input being recorded for the remainder of the cycle.

It was necessary to design the switching arrangement so that the L.V.D.T. and thermocouple circuits are completely independent. The switching may be accomplished with only one switch if a common line is maintained between the two input circuits and the recorder. However, it was found that with such an arrangement the L.V.D.T. voltage was affected by the thermocouple voltage when the latter was greater than about 10 millivolts.

3. The Sample Holder

The sample may be contained in an open crucible for free vaporization experiments, or in a closed cell with a small orifice (Knudsen cell) for equilibrium vapor pressure measurements. The most convenient type of open cell was found to be a cup made from quartz tubing, shown in figure 11a. The type of Knudsen cell used is shown in figure 11b. It is made of stainless steel rod which was formed on a lathe into a tapered cup and lid. A quartz liner is used to reduce reaction of the sample with the cell and to facilitate cleaning of the sample holder. A second type of Knudsen cell, shown in figure 11c, was made from a rod of compressed boron nitride. In this type, the lid screws onto the cup. In both types of Knudsen cell, the thickness of the lid in the vicinity of the orifice was made as small as the mechanical strength of the material would permit.

C. TEMPERATURE CONTROL AND MEASUREMENT

The temperature of the sample is controlled above room temperature with an electric resistance furnace. The furnace encloses that part of the centre vacuum jacket which contains the top of the spring balance and the sample.

The furnace is constructed so that it may be removed easily with minimum disturbance to the rest of the apparatus. The vacuum need not be broken, but weight measurement must be temporarily interrupted since manipulation of the furnace

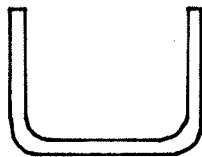
FIGURE 11

THERMOGRAVIMETRIC APPARATUS

Sample Holders

- (a) Open cell - quartz or "Vycor"
brand glass
- (b) Knudsen cell - stainless steel
- (c) Knudsen cell - compressed boron
nitride

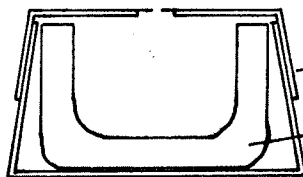
Scale: 2X



1.0 mm. wall
"Vycor" or
quartz tubing

(a)

Scale: 4X

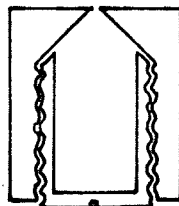


stainless steel

quartz liner

(b)

Scale: 2X



compressed
boron nitride

(c)

causes the spring balance to vibrate.

The furnace consists of two half-cylindrical heating elements surrounded by brick insulation (see figure 12). The bricks are held in a tray made from $\frac{1}{4}$ inch asbestos sheet. This whole assembly is supported by two bricks resting on the bench top. The heating elements were obtained from Electro Applications, Inc., 2439 West Pike Street, Houston, Pennsylvania. They are in the form of helically wound coils of an iron-chromium-aluminum alloy wound on a ceramic form and covered with an alumina cement. Their maximum recommended operating temperature is 1210° C.

The heating elements and insulating bricks are fitted together but not cemented. The furnace is removed from the apparatus simply by removing each brick and element in turn.

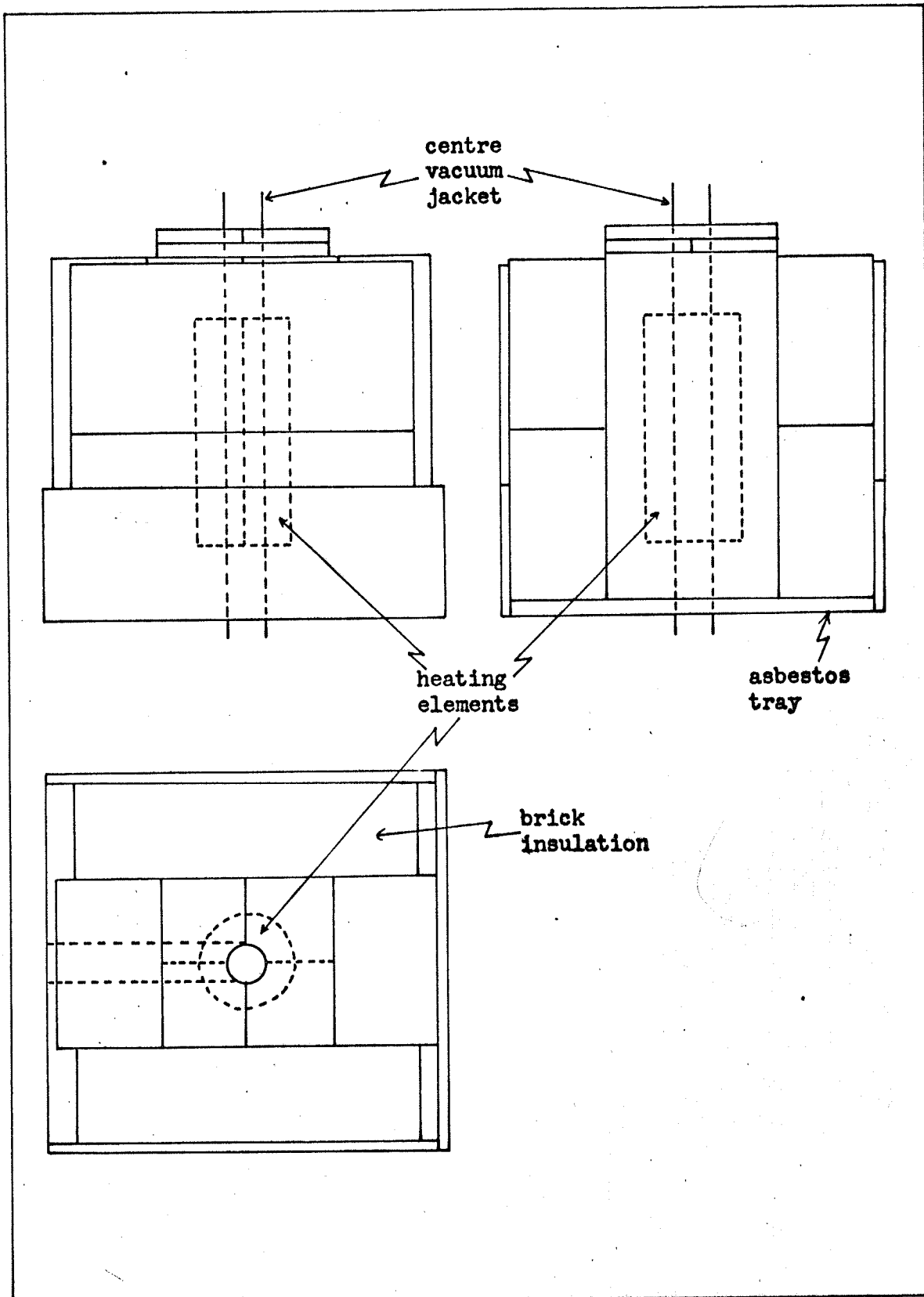
The voltage supplied to the furnace is controlled by a variable transformer. The model used is a "Powerstat 136B" supplied by the Superior Electric Company, Bristol, Connecticut. It has an output voltage variable from 0 to 110 volts and a maximum current rating of 22 amps. A Hurst model "C" 1 r.p.m. reversible A.C. motor is used with a locally made gear system to turn the variable transformer through one revolution in approximately five hours.

The temperature of the atmosphere in the vicinity of the sample is measured with Chromel-Alumel thermocouples. Two independent thermocouples are used. The cold junctions

FIGURE 12

THERMOGRAVIMETRIC APPARATUS

Construction of the Furnace



are placed in an ice-water bath and the hot junctions are arranged so that one is just above and one is just below the sample, (see figure 6, page 57). The distance of the junctions from the sample holder is approximately 0.2 centimeters and from each other is approximately 1 centimeter. This arrangement was chosen so that some measure of the temperature gradient in the vicinity of the sample could be obtained.

D. PRESSURE CONTROL AND MEASUREMENT

The entire spring balance assembly is enclosed in a glass vacuum jacket which is evacuated with a rotary pump and an oil diffusion pump. The pressure is measured with a thermocouple gauge placed in that part of the vacuum system which is furthest away from the diffusion pump.

The vacuum jacket consists of upper, centre and lower portions which fit together with ground glass tapered joints (see figure 6, page 57). The upper vacuum jacket is made of pyrex brand glass and contains a female ground glass taper. The removable male part of this joint contains the vacuum seal for leading in the thermocouple wires. The seal was made by filling the space between the wires and the inside of the male taper with silicon rubber cement. This arrangement was found to provide a vacuum seal which is at least as good as the ground glass joints used in the rest of the vacuum system.

The centre vacuum jacket is made of "Vycor" brand glass tubing which has thermal properties similar to those of quartz. It surrounds the upper part of the spring balance yoke and the sample. It is around this part of the vacuum jacket that the furnace is fitted.

The lower vacuum jacket is made of "Pyrex" brand glass and is connected directly to the glass vacuum line leading to the vacuum pumps and the thermocouple gauge. It contains the centre and lower parts of the spring balance and the L.V.D.T. core.

With the furnace at 1000° C, the joint between the centre and upper vacuum jackets was found to be too hot to touch but did not leak. The joint between the centre and lower vacuum jackets, however, was found to be close enough to the furnace to require water cooling.

EXPERIMENTAL PROCEDURE

PART SIX: EXPERIMENTAL PROCEDURE

A. GENERAL

Knudsen cell and free vaporization experiments were performed on each of the compounds: TiSe_2 , VSe_2 , Cr_2Se_3 , ZrSe_2 , MoSe_2 , TaSe_2 and WSe_2 . The experiments were performed in two series. The first included Knudsen cell and free vaporization experiments performed at a minimum heating rate. The second series consisted entirely of free vaporization experiments performed at a linear rate of heating.

Before these experiments are described, the procedure for calibration of the thermobalance is given.

B. CALIBRATION OF THE THERMOBALANCE

Before each series of experiments, a relatively complex calibration procedure was performed. For the first series of experiments, the procedure consisted principally of adjusting the calibration controls included in the design of the thermobalance. However, after this series was complete, a number of factors were identified which were affecting the weight reading. Steps to compensate for these new factors were added to the calibration procedure used for the second series of experiments.

Undesirable variations in the weight reading due to electrical factors were for the most part accounted for in the design of the circuitry of the weight measuring system.

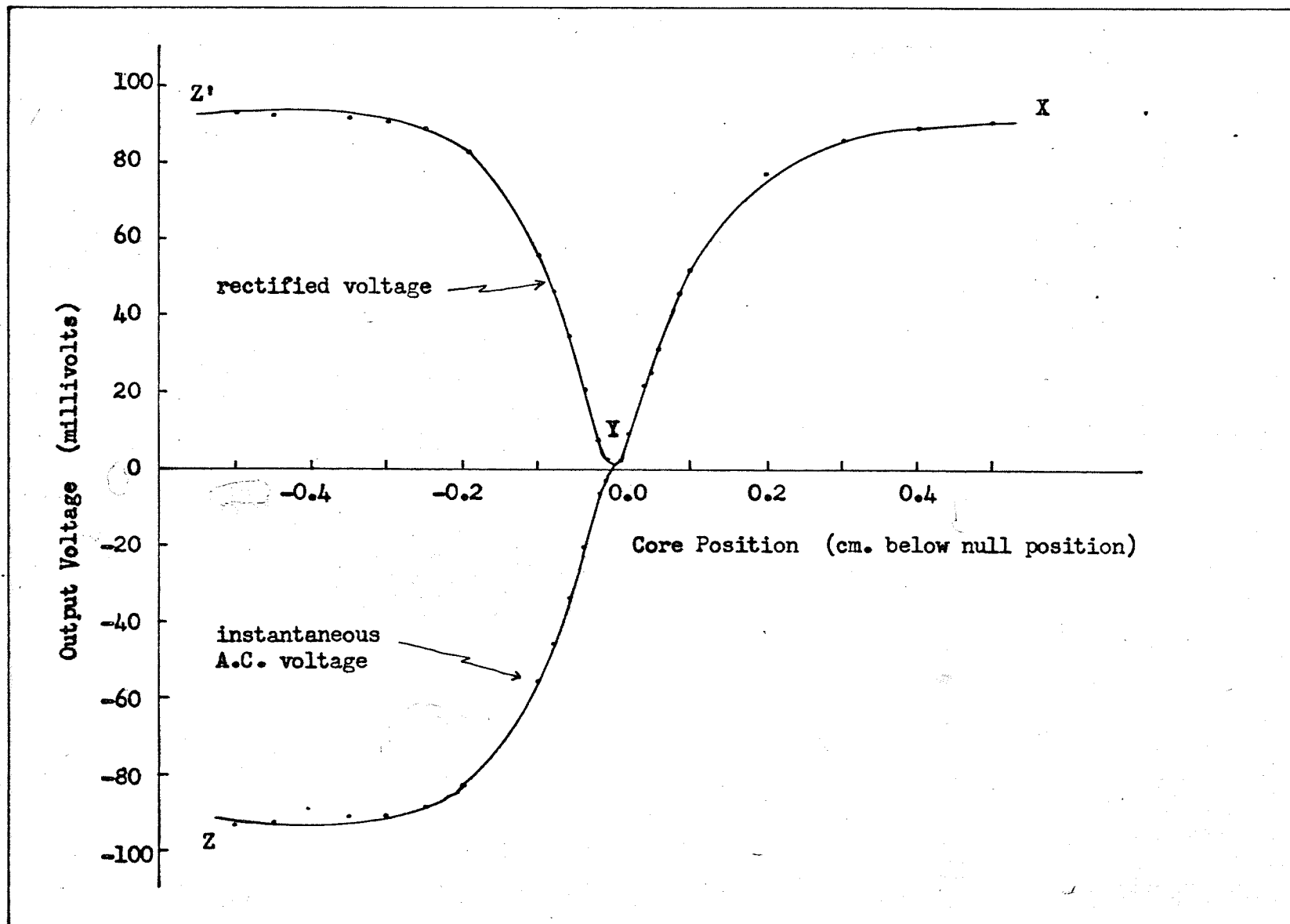
For example, the L.V.D.T. input circuit, the amplifier-rectifier and the chart recorder each contain their own voltage regulating circuits which prevent their performance from being significantly affected by fluctuations in the line voltage. However, some undesirable variations in the weight reading were traced to mechanical factors. For example it was found that the horizontal bar supporting the quartz spring was sufficiently bent that rotating it about its long axis changed the weight reading by approximately 5%. A similar effect resulted from small changes in the position of the spring on the horizontal bar. These components are shown in figure 7, page 59.

It is convenient to explain the calibration procedure by reference to the response curve of the L.V.D.T.. This curve is shown in figure 13 as a graph of L.V.D.T. output voltage as a function of core position. Points X, Y and Z in figure 13 correspond, respectively, to positions A, C and B in figure 8, page 63. Although the instantaneous voltage at the output of the L.V.D.T. (curve XYZ in figure 13) changes polarity as the core passes position Y, the subsequent rectification of this A.C. voltage makes the D.C. input to the chart recorder insensitive to the phase change. Thus the input to the chart recorder remains positive with a minimum value at position Y, the null point of the L.V.D.T., and is represented by the curve XYZ' in figure 13.

FIGURE 13

L.V.D.T. RESPONSE CURVE

Output voltage vs. core position



The calibration procedure consists of adjusting the positions of the horizontal bar and the quartz spring to a reproducible reference point and adjusting the calibration controls so that the balance is operating on a linear part of the L.V.D.T. response curve. In addition, the range of the output voltage is set for a value which is suitable for the sample and the chart recorder. Fortunately, the null point of the L.V.D.T. provides a convenient reference point and is also in the vicinity of a linear part of the response curve. Figure 14 shows the L.V.D.T. response curve in the region of the null position.

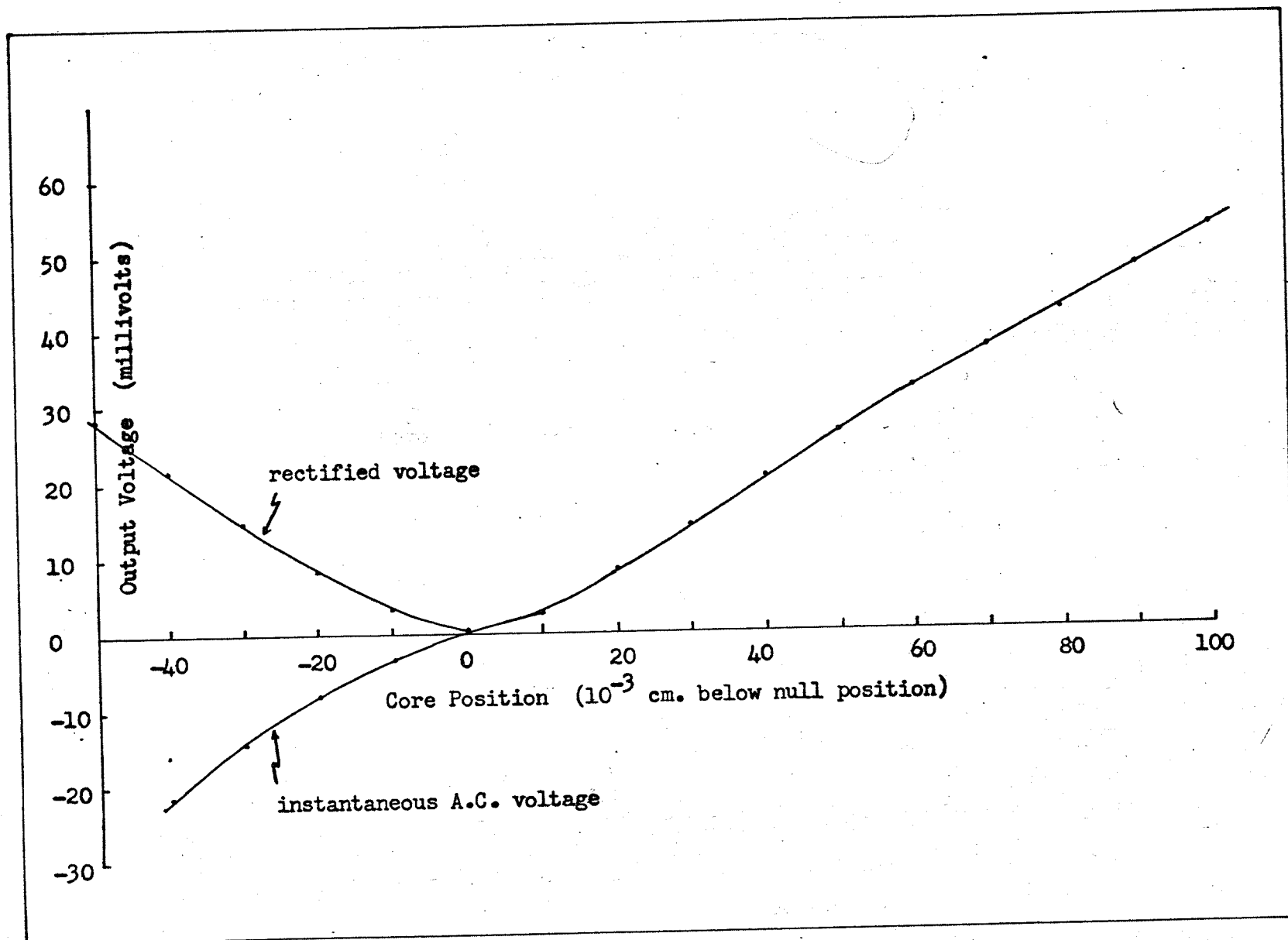
In detail, the calibration is performed in the following steps:

1. The empty sample holder to be used is placed on the balance.
2. The L.V.D.T. solenoid, the horizontal bar and the quartz spring are adjusted so that the core is in the null position, as indicated by a minimum weight reading on the chart recorder.
3. The zeroing voltage provided by the L.V.D.T. amplifier is adjusted so that the L.V.D.T. null voltage corresponds to a reading of zero on the chart recorder.
4. A known weight close to the weight of the sample (usually 100 mg.) is placed in the sample holder and the 3K potential divider, which controls the voltage fed to the

FIGURE 14

L.V.D.T. RESPONSE CURVE CLOSE TO NULL POSITION

Output Voltage vs. Core Position



recorder from the amplifier, is adjusted so that the recorder reading corresponds to the known weight.

5. The weight is removed from the sample holder and the zero setting is checked.

C. THERMOGRAVIMETRIC EXPERIMENTS

1. Introduction

Two series of experiments were performed. In the first, samples of each of the compounds were subjected to a temperature program similar to that shown in figure 15a. This is the minimum heating rate which can be provided by the gears available to drive the variable transformer which controls the furnace voltage. Both Knudsen cell and free vaporization experiments were included in this first series. In the second series, free vaporization experiments were conducted using the linear temperature program shown in figure 15b. In both series of experiments, the sample weight and the furnace temperature were continuously recorded as functions of time.

The samples were supplied by Cerac, Inc., Box 126, Butler, Wisconsin. They were used as received with no further purification.

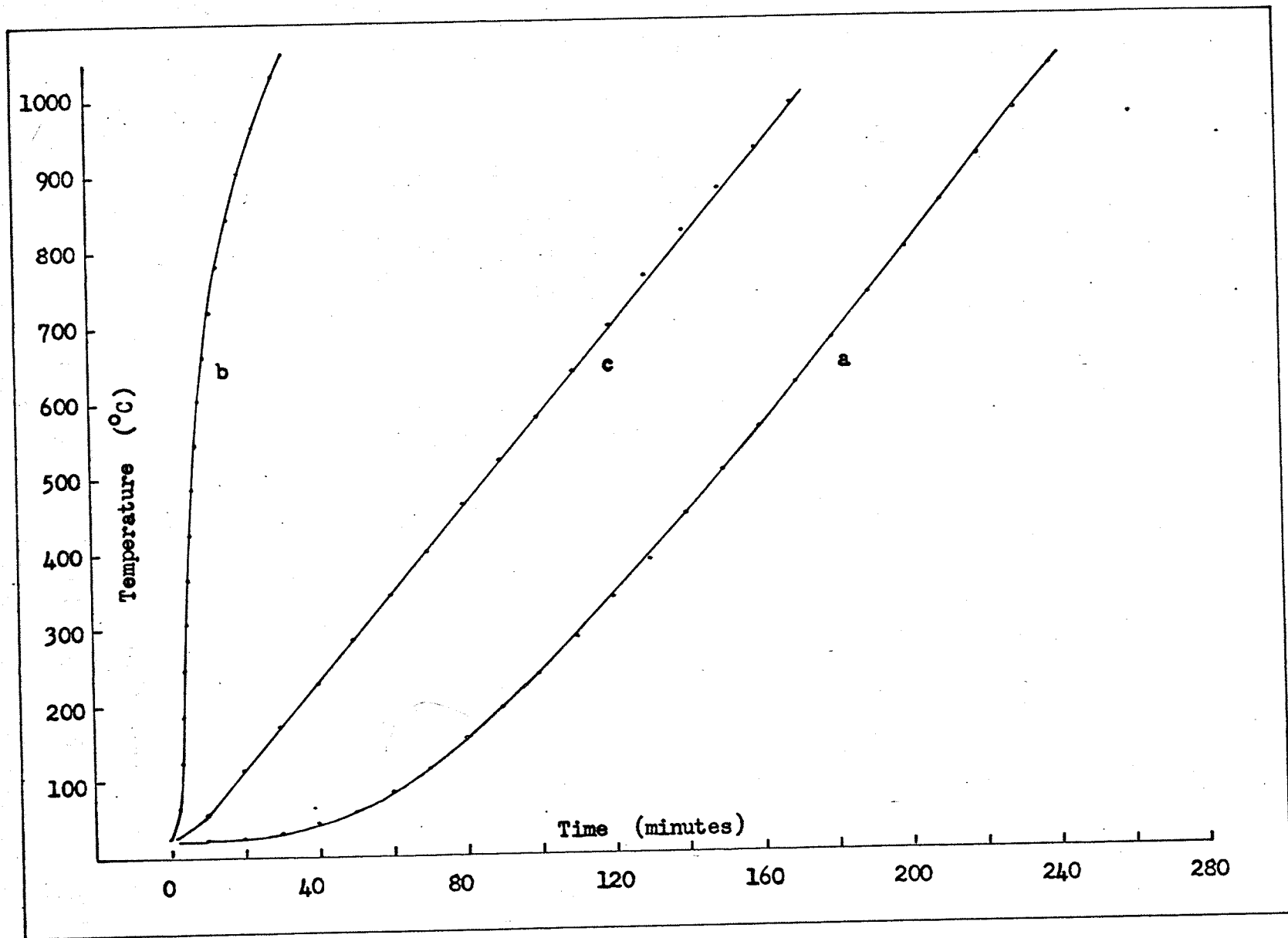
2. Minimum Heating Rate Experiments

In the Knudsen experiments, the cells used were made of stainless steel and had quartz liners (see figure 11b, page 74). The orifices were made with a 0.018 inch

FIGURE 15

FURNACE TEMPERATURE PROGRAMS

- (a) Minimum heating rate
- (b) Maximum heating rate
- (c) Linear heating program



diameter drill and therefore probably had a diameter somewhat greater than this. The orifice dimensions were not determined more accurately since other factors precluded the use of the results of this series of experiments from yielding accurate vaporization rates.

In a typical Knudsen cell experiment, approximately 100 mg. of a sample was weighed to ± 0.1 mg. into a quartz liner. The liner was placed in the cell and the lid was pushed on. The cell was placed on the thermobalance yoke, the centre and upper vacuum jackets were put in place using Dow Corning silicone stopcock grease to make vacuum seals at the ground glass joints, and the apparatus was evacuated with the rotary and oil diffusion pumps. When a vacuum of approximately 10^{-4} mm. Hg, as indicated by the thermocouple gauge, had been reached, the furnace assembly was put in place. The variable transformer which controls the furnace voltage was set at an initial value between 0 and 5 volts. The thermocouple reference junctions were placed in an ice-water bath and the recorder chart speed was set for approximately 5 inches per hour. With the recorder on, the variable transformer motor and the furnace voltage were switched on simultaneously and allowed to run until the thermocouples indicated a furnace temperature of 1000° C, when the furnace power and the motor were switched off. Throughout the experiment, the L.V.D.T. output was recorded

continuously except for 30 second intervals spaced 10 minutes apart during which the furnace temperature was recorded.

In some cases, compounds which indicated a significant weight change during this series of Knudsen cell experiments were subjected to further experiments in which they were heated in Knudsen cells and in open "Vycor" crucibles at a constant temperature of 1000° C until no further weight change was observed. In these experiments, the samples were brought as quickly as possible to 1000° C by turning the variable transformer to the maximum setting before switching on the furnace voltage. The heating program which resulted is shown in figure 15b.

At the end of each experiment, the furnace power was switched off and the apparatus was allowed to return to room temperature over a period of several hours. During the cooling period it was necessary to maintain the vacuum since the thermocouples and the stainless steel cells were found to oxidize rapidly in air at high temperatures.

When the apparatus had cooled to room temperature, the furnace assembly and the upper and centre vacuum jackets were removed and the sample holder plus residue was weighed to ± 0.1 mg. on an analytical balance. The sample residue was then removed and the cell re-weighed to determine whether there had been any change in its weight during the experiment. Unfortunately, in the case of Knudsen cells,

the lids were usually very difficult to remove, especially after experiments involving prolonged heating at high temperature. In several cases the cell was damaged or destroyed in attempting to open it. In such cases it was not possible to confirm that the net weight change represented the change in the weight of the sample.

Blank experiments were performed using the same procedure but with a piece of Chromel wire of the same weight to replace the sample. These blank experiments showed that there was considerable drift in the weight reading as the temperature was increased. Attempts to eliminate this drift were unsuccessful and it was found to be insufficiently reproducible to apply an accurate correction to the results of the minimum heating rate experiments.

3. Linear Heating Rate Experiments

A more reproducible weight drift was eventually obtained by (a) carefully adjusting to a reference point the positions of the quartz spring and the horizontal bar as described in the calibration procedure, and (b) changing the heating program to one which was linear for as much of the heating time as possible but which still provided a low heating rate. It was found that by using an initial setting for the variable transformer of 26.5% but turning it at the same speed as before, the linear heating program shown in figure 15c was obtained. This curve represents a heating rate of 5.85° C per minute.

This second series of experiments consisted entirely of free vaporizations of each of the compounds using the "Vycor" crucibles shown in figure 11a page 74. The details of the experimental procedure are the same as those given for the Knudsen cell experiments except that (a) the improved calibration procedure and the linear heating program were used and (b) at the end of the linear temperature program, the furnace voltage was reduced to maintain the temperature at $1000^{\circ} \text{C} \pm 5^{\circ} \text{C}$ by periodically adjusting the variable transformer setting by hand to compensate for fluctuations in the line voltage and the room temperature.

During the first series of experiments, the sample temperature was measured with two thermocouples, one hot junction being placed just above the cell and the other just below as described in part 2c of this chapter. However, it was found that at no point in the temperature range of 25°C to 1000°C was there a difference of more than 5°C between the indications of the two thermocouples. For the second series of experiments, only one thermocouple was used. This was arranged so that when the upper and centre vacuum jackets were in place, the hot junction was centred over and approximately 0.5 cm. above the surface of the sample.

RESULTS

A. GENERAL

The results of the Knudsen cell experiments are presented together with those free vaporization experiments which were carried out with the minimum heating rate temperature program. This arrangement was chosen rather than presenting the results of the Knudsen experiments separately from the free vaporization experiments because the lack of reliable drift correction for the entire first series of experiments meant that the weight curves obtained could provide only a rather limited amount of information. This information can most easily be presented in tabular form.

Since a linear heating program was used for the second series of experiments, a reproducible correction curve for the weight drift could be obtained. The corrected results of these experiments are therefore presented as graphs of sample weight vs. temperature and sample weight vs. time at constant temperature. All of the second series of experiments were of the free vaporization type.

B. MINIMUM HEATING RATE EXPERIMENTS

Since a reliable drift correction was not obtained for the temperature program used in the first series of experiments, the information obtained from this series is somewhat limited. In particular, vaporization rates could not be measured since the actual rate of weight loss could not be separated from the apparent rate of weight loss caused by

the drift in weight reading with temperature. However, even though the shape of the drift curve varied from experiment to experiment, it was always smoothly varying with no sudden discontinuities. It was therefore possible to note relatively sudden dips in the weight curves of samples which underwent a significant degree of decomposition. In addition, the total weight change during an experiment could be determined by weighing the sample holder on an analytical balance before and after each run.

The results obtained from the first series of experiments are listed in table 3. The table contains the following information:

Column 1: a reference number for the experiment.

Column 2: the formula of the compound as quoted by the supplier.

Column 3: the type of temperature program used. For the TiSe_2 experiments at constant temperature (M2 and M3) the temperature was initially attained by the rapid heating program shown in figure 15b page 91. All the other experiments in this table were conducted at low heating rates with temperature curves similar to that shown in figure 15a, the data for which were taken from the Cr_2Se_3 experiment in this series. This column shows the time required to raise the temperature from room

TABLE 3

RESULTS OF MINIMUM HEATING RATE EXPERIMENTS

(Effusion cell experiments except as noted. All in vacuum)

Experi- ment Number	Com- pound	Time to reach 1000° C (min.)	Sample Weight		Final Compo- sition (n in MSe _n)	First Dip in Weight Curve	
			Init- ial (mg.)	Total Change (% of init.)		Temp. (° C)	Size (div.)
M1	TiSe ₂	228	91.0	-2.3	1.940	254	5.2
M2	TiSe ₂	*	91.0	-10.4	1.729	-	-
M3	TiSe ₂	**	93.3	-25.0	1.348	-	-
M4	VSe ₂	225	94.1	-3.7	1.902	293	2.9
M5	VSe ₂	*** 235	100.1	-4.1	1.892	177	3.7
M6	Cr ₂ Se ₃	231	92.0	**** -8.2	**** 1.146	none	observed
M7	ZrSe ₂	227	92.7	-1.6	1.949	236	0.7
M8	MoSe ₂	237	99.4	-0.3	1.990	none	observed
M9	TaSe ₂	215	90.1	-1.7	1.927	307	1.5
M10	WSe ₂	233	96.0	-0.2	1.991	none	observed

* Heated at 1044 ± 10° C for 25 hours.

** Free vaporization. Heated at 1015 ± 10° C for 30 hours.

*** Free vaporization. Pre-heated in vacuum at 60° C for 11 hours during which chart recorder indicated no weight change.

**** Calculated from increase in weight of sample holder.

temperature to 1000° C and indicates the variation in the temperature programs of the different experiments in this series. This variation was caused by failure to set the variable transformer to the same initial value for each experiment.

Column 4: the initial weight of the sample.

Column 5: the difference between the initial and final weights of the sample expressed as a percentage of the initial weight.

Column 6: the composition of the sample after the experiment expressed as the number of selenium atoms per molecule. This figure was calculated assuming the original sample had the molecular formula given in Column 1, that the total weight loss was due entirely to loss of selenium and that this loss of selenium occurred homogeneously throughout the sample.

Column 7
and 8: the temperature at which the first significant dip in the weight curve appeared and its magnitude. The drift in weight reading with temperature prevented accurate calibration of the weight reading in milligrams. However, the dips in the weight curves occurred at low temperatures where the drift is not large (see figure 23, page 117) and since the initial calibration was made so

that 100 recorder divisions equalled approximately 100 mg. the figures quoted in column 8 in divisions may be taken to be approximately equivalent to milligrams. Further, since the samples initially weighed between 90 and 100 mg. the column 8 figures also represent approximate weight percentages and may be compared directly with the figures in column 5.

It was found that when the total weight loss of the sample was more than 1.5 mg., a deposit of bright red elemental selenium could be observed at the ends of the centre vacuum jacket. An exception was the case of Cr_2Se_3 in experiment M6 for which the total loss in weight is listed as 8.2 weight % but no selenium was observed. In this experiment, there was no change in the total weight of the sample plus the cell. However, when the cell was opened after the experiment, a grey, scaly deposit was found on the inside walls of the stainless steel. After the loose residue of the sample was removed, the cell was weighed and found to have increased in weight by 7.5 mg. during the experiment. Since there had been no change in the weight of the sample plus the cell, it was concluded that the sample had lost weight by 7.5 mg..

C. LINEAR HEATING RATE EXPERIMENTS

The results of the free vaporization experiments

using a linear heating program are presented in graphical form in figures 16 to 22 inclusive. Each figure contains two graphs:

(a) a plot of weight versus temperature at a linear heating rate of 5.85° C per minute, and

(b) a plot of weight versus time at a constant temperature of 1000° C.

The two graphs obtained for each compound are shown on the same diagram since they were both obtained during the same experiment (see Apparatus and Procedure, page 95.) In each case the point at 1000° C on graph (a) is the same as that at zero minutes on graph (b).

The first part of the heating program, from room temperature to 1000° C, used for each of the experiments in this series did not differ from that shown in figure 15c by more than $\pm 5^{\circ}$ C at any point. During the constant temperature part of each experiment, the temperature was kept at 1000° C $\pm 5^{\circ}$ C.

The results of a blank run under these conditions are shown in figure 23 as graphs of recorder reading versus temperature and versus time.

The weight readings in figures 16 to 22 were obtained in the following way: Corrections from the results of the blank experiments were added to the uncorrected chart recorder readings at corresponding temperatures and times.

FIGURE 16

FREE VAPORIZATION OF TiSe_2 IN VACUUM

(a) Weight vs temperature at $5.85^\circ \text{C}/\text{min}$.

(b) Weight vs time at 1000°C

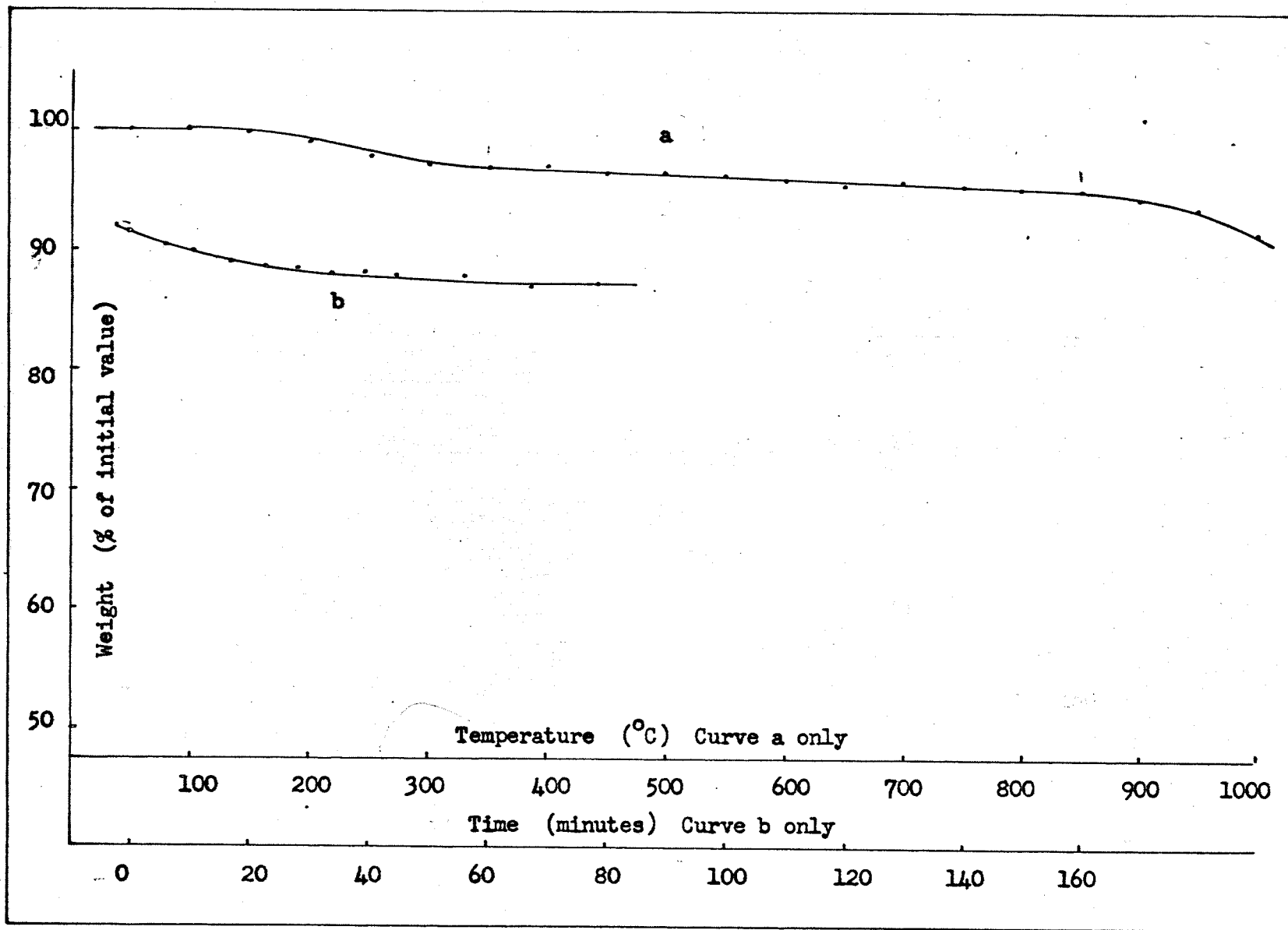


FIGURE 17

FREE VAPORIZATION OF VSe_2 IN VACUUM

(a) Weight vs temperature at $5.85^\circ C/min.$

(b) Weight vs time at $1000^\circ C$

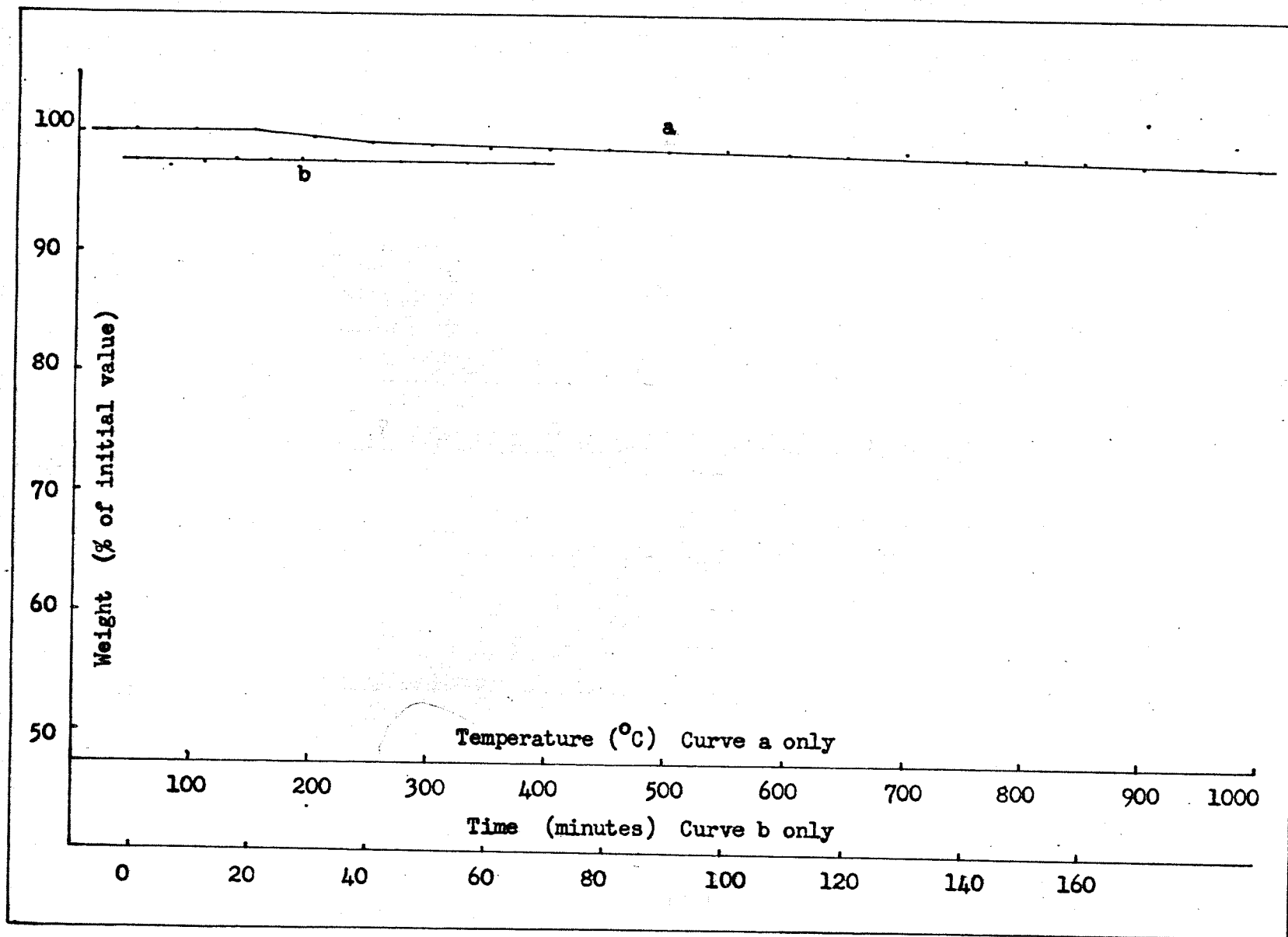


FIGURE 18

FREE VAPORIZATION OF Cr_2Se_3 IN VACUUM

- (a) Weight vs temperature at 5.85°C/min.
- (b) Weight vs time at 1000°C

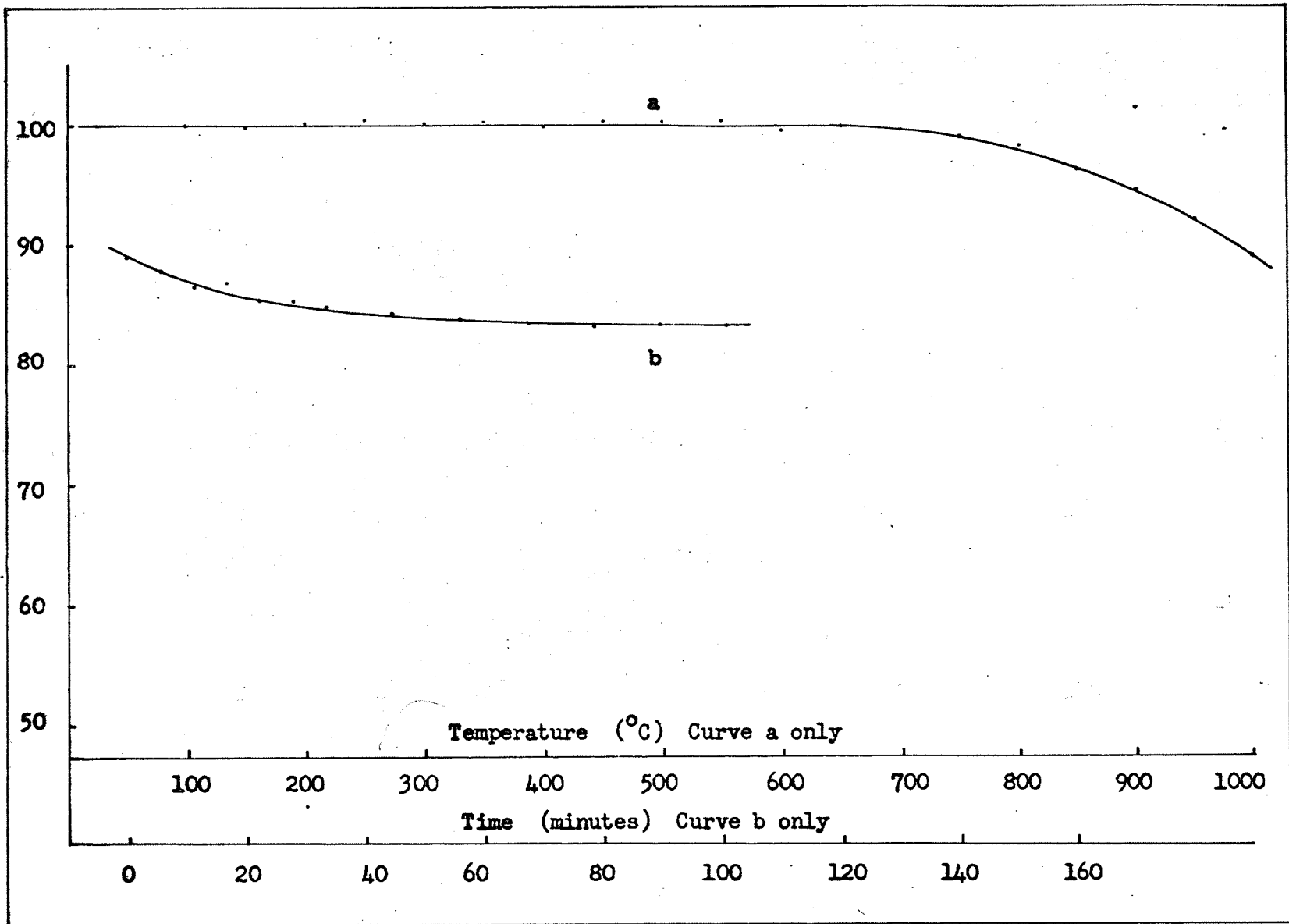


FIGURE 19

FREE VAPORIZATION OF $ZrSe_2$ IN VACUUM

(a) Weight vs temperature at $5.85^\circ C/min.$

(b) Weight vs time at $1000^\circ C$

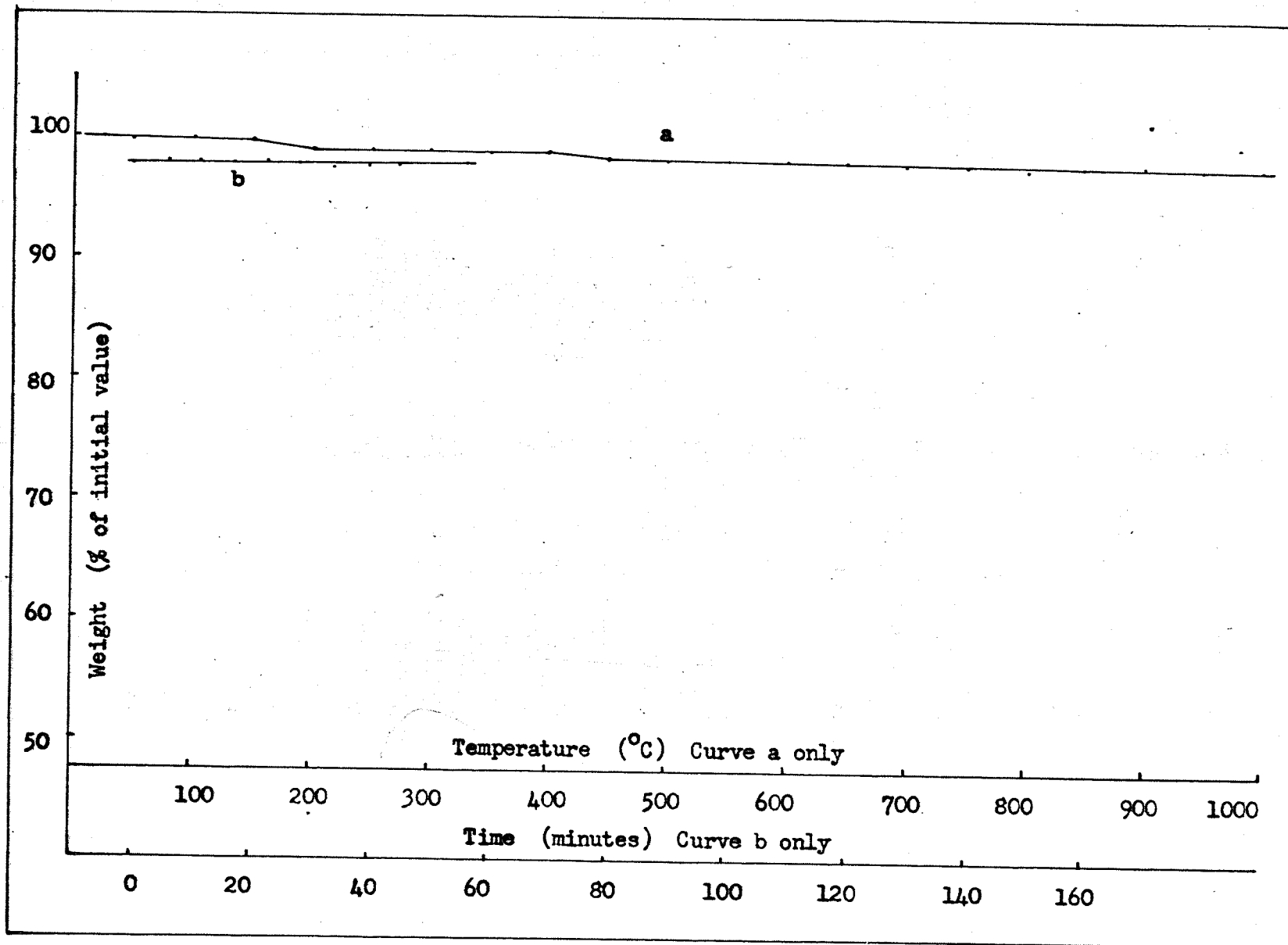


FIGURE 20

FREE VAPORIZATION OF MOSe_2 IN VACUUM

(a) Weight vs temperature at $5.85^\circ \text{C}/\text{min}$.

(b) Weight vs time at 1000°C

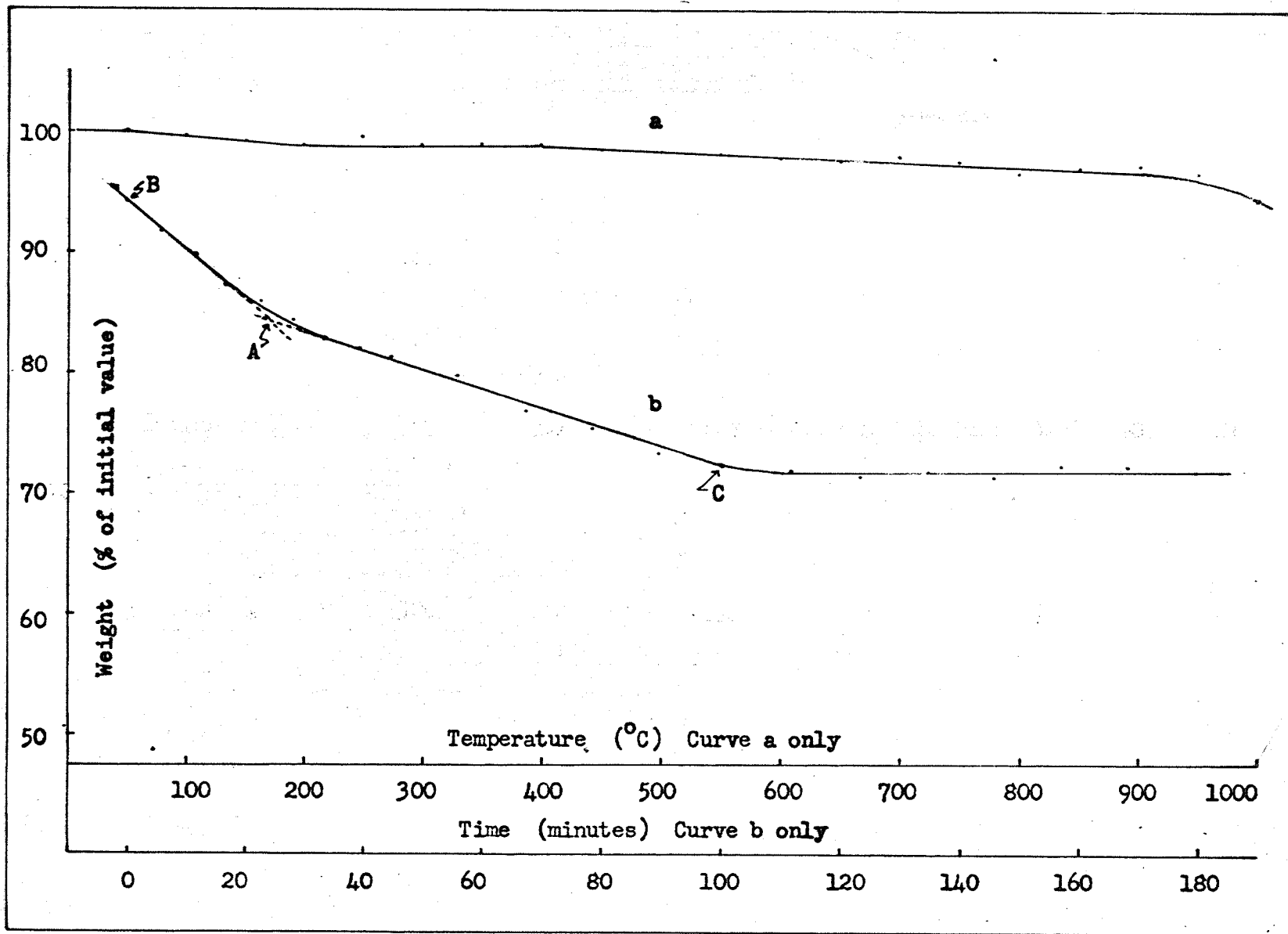


FIGURE 21

FREE VAPORIZATION OF TaSe_2 IN VACUUM

- (a) Weight vs temperature at 5.85°C/min.
- (b) Weight vs time at 1000°C

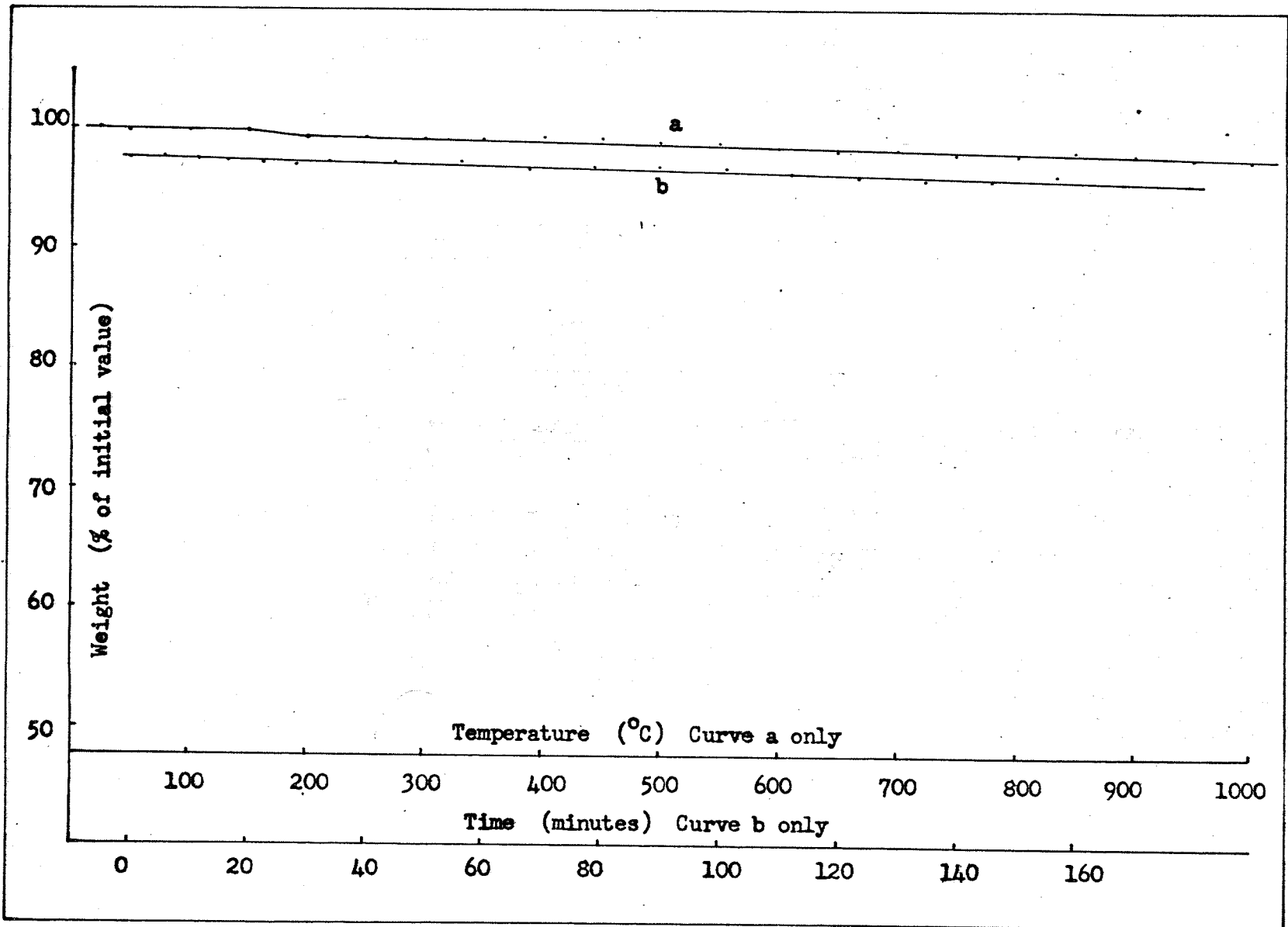


FIGURE 22

FREE VAPORIZATION OF WSe_2 IN VACUUM

- (a) Weight vs temperature at 5.85°C/min.
- (b) Weight vs time at 1000°C

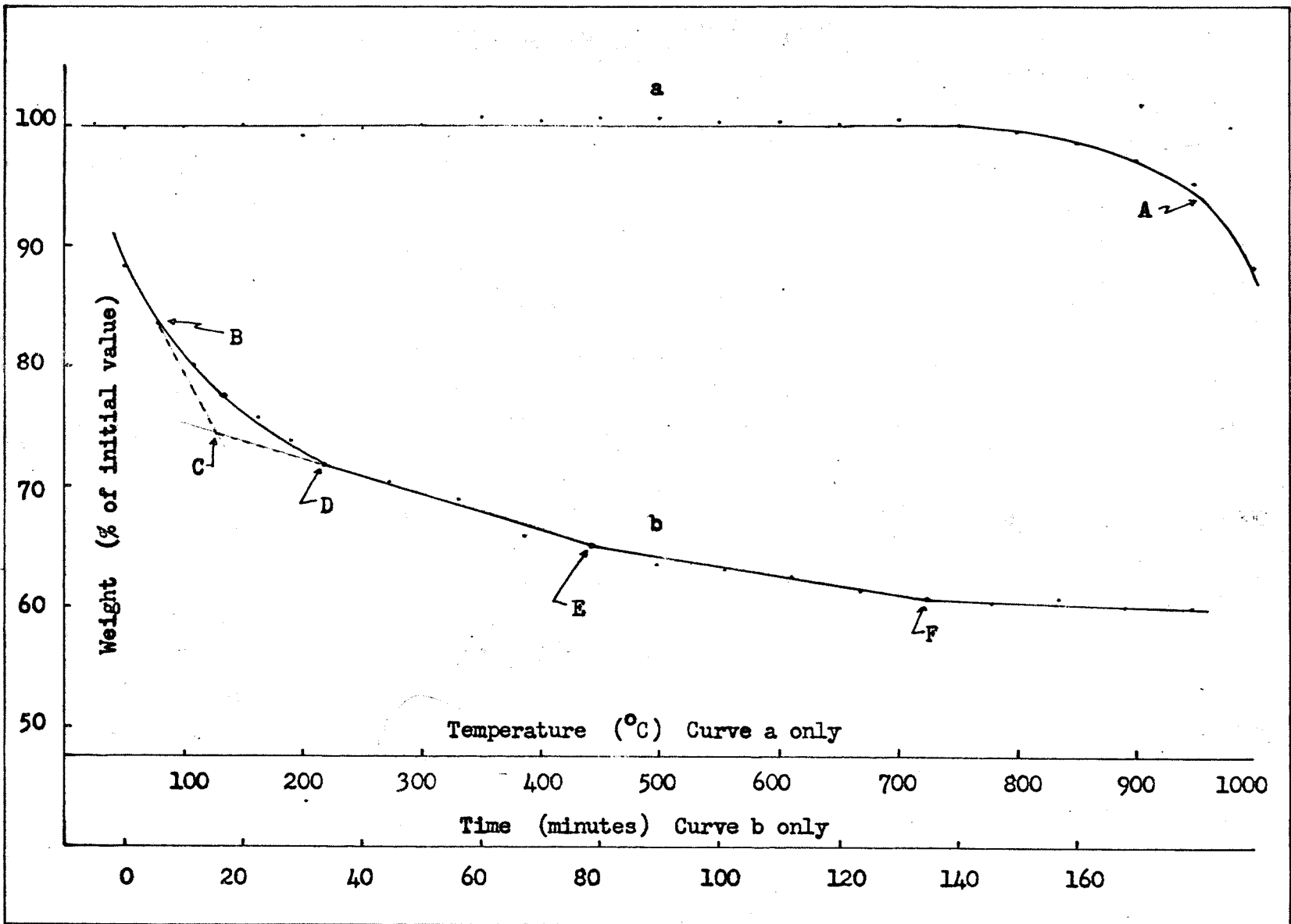
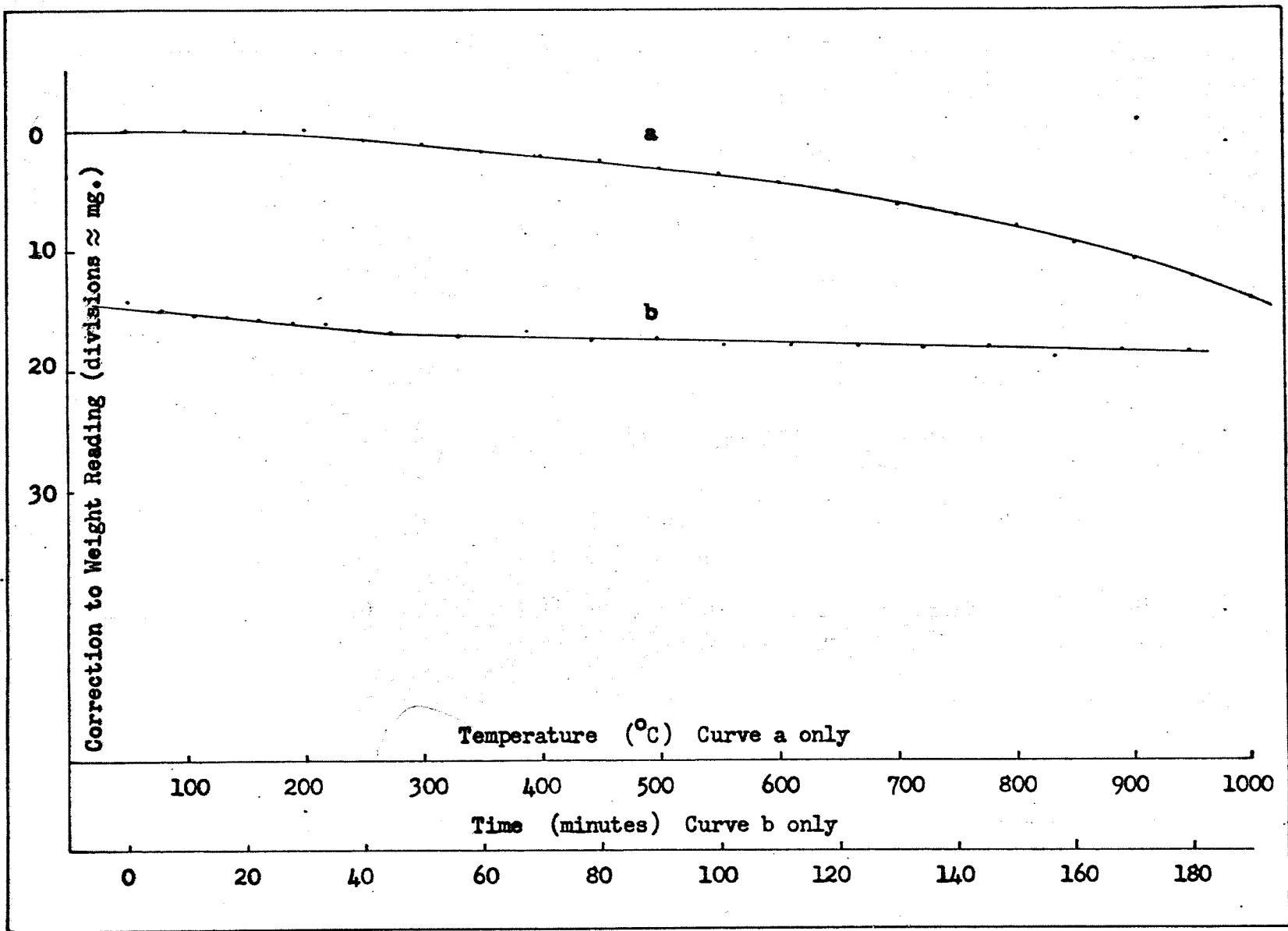


FIGURE 23

CORRECTION FOR DRIFT IN WEIGHT READING

- (a) Weight vs temperature at 5.85° C/min.
(see figure 15c)
- (b) Weight vs time at 1000° C



The corrected chart readings in divisions were converted to sample weights in weight percent by, (a) setting the initial chart reading equal to 100%, (b) setting the final corrected chart reading equal to the final weight of the sample (as determined by weighing the residue on an analytical balance after the experiment) expressed as a weight percentage of the initial sample weight, and (c) assuming a linear correspondence of corrected recorder reading to sample weight.

The empty "Vycor" crucible was weighed before and after each experiment. In no case did the two weights differ by more than ± 0.1 mg.

The results of the linear heating rate experiments are summarized in table 4.

TABLE 4

RESULTS OF LINEAR HEATING RATE EXPERIMENTS

(Free vaporizations in vacuum)

<u>Experi- ment Number</u>	<u>Com- pound</u>	<u>Sample Weight</u>		<u>Final Compo- sition (n in MSe_n)</u>	<u>First Dip in Weight Curve</u>	
		<u>Init- ial (mg.)</u>	<u>Change (% of init.)</u>		<u>Temp. (° C)</u>	<u>Size (% of init. wt.)</u>
L1	TiSe ₂	91.0	-13.2	1.656	140	3.0
L2	VSe ₂	90.6	-2.4	1.937	150	1.2
L3	Cr ₂ Se ₃	90.9	-16.8	0.775	640	16.8
L4	ZrSe ₂	91.0	-2.2	1.931	150	0.6
L5	MoSe ₂	90.7	-28.3	1.090	900	25.3
L6	TaSe ₂	90.9	-4.4	1.811	150	0.6
L7	WSe ₂	91.1	-40.1	0.264	750	40.1

DISCUSSION

A. GENERAL

The experimental results obtained in this study are discussed with respect to the thermal stabilities of the compounds investigated and the decomposition reactions which each appeared to undergo. The decomposition reactions are compared with the reported stable phases in each of the metal-selenium systems.

Vaporization rates could not be calculated from the effusion cell experiments due to drift in the L.V.D.T. weight reading. However, even if a correction for this had been available, vaporization rate measurements would probably have been quite inaccurate due to the generally small amounts of dissociation occurring. An added inaccuracy in the calculation of vapor pressure would have been the uncertainty in the orifice dimensions. The difficulty of removing the lid of the cell without damage after prolonged heating at 1000° C would have in several cases prevented the calibration of the cell with a substance of known vapor pressure. Successful effusion cell experiments on these compounds will probably require longer periods of measurement with unreactive, re-usable cells such as the boron nitride design suggested in the Introduction. In addition, the need to know the molecular weight of the vapor suggests that these compounds should also be studied by a technique such as mass spectrometry.

The free vaporization experiments were not used to calculate vapor pressures because of the large uncertainty in the surface area of the polycrystalline samples and lack of knowledge of the identity of the vapor. In addition, some trial calculations using vaporization rates given by the slopes of the linear portions of the WSe_2 and $MoSe_2$ weight curves yielded values of $P_e - P$, where P_e is the vapor pressure of the compound and P is the external pressure on the sample, between 0.68×10^{-4} mm. Hg and 8.7×10^{-4} mm Hg. These calculations were based on the assumptions that the sample area was 0.79 cm^2 , the area of the bottom of the cell, and that the vapor was entirely Se_2 . The fact that $P_e - P$ is of the same order as the external pressure, P , together with the fact that P was not accurately measured suggest that useful values of P_e cannot be obtained from this experimental information.

B. THERMAL STABILITIES

For the purpose of this discussion the thermal stability of a sample is defined as that temperature at which the first significant change in its weight occurs. The degree of significance of any particular weight change was determined by comparing it with the total weight change during the experiment. According to this definition, the thermal stabilities of the compounds studied are given in Column 7 of table 3 and Column 6 of table 4.

The results of both the Knudsen cell and free vaporization experiments indicate that the selenides of the group VI metals are far more stable than those of groups IV and V. Within group VI the order of stability appears to be $Mo > W > Cr$. However, within groups IV and V, the differences in the stability temperatures obtained for a given type of experiment are considered to be too small to justify arranging the compounds in any particular order of stability. The temperatures assigned to the dips in the Knudsen experiment weight curves may contain errors due to the drift in the weight reading and there seems good reason to ascribe initial weight losses occurring near $143^{\circ} C$ in the free vaporizations to loss of uncombined selenium (see part C of discussion).

C. DECOMPOSITION REACTIONS

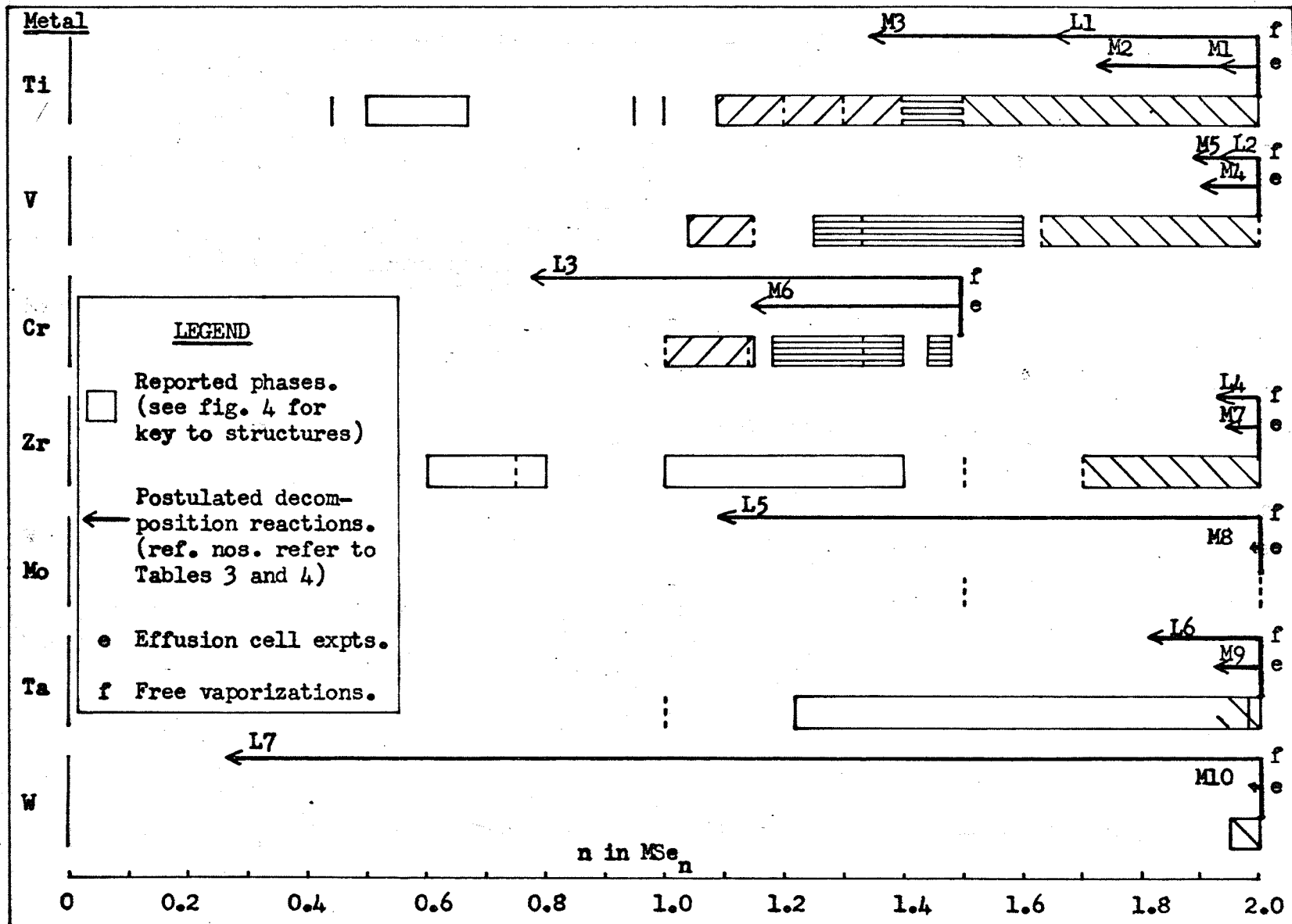
The weight changes measured in this study are discussed here in relation to the phases which have been previously reported in each of the metal-selenium systems. In order to facilitate the discussion, the compositions of the original samples and the calculated compositions of the final products are shown in figure 24 superimposed on the relevant parts of the one-dimensional phase diagrams. The sources of information for these phase diagrams are listed in table 1, page 18.

The tables and figures relevant to a particular part

FIGURE 24

POSTULATED DECOMPOSITION REACTIONS

Apparent changes in composition shown in relation
to phases previously reported



of the discussion are listed with its heading.

1. Effusion Cell Experiments (see table 3 and figure 24)

Except for Cr_2Se_3 and TaSe_2 , none of the effusion cell experiments resulted in decompositions which correspond to transitions between different phases. The decompositions observed for MoSe_2 and WSe_2 were almost negligible since no free selenium was observed during the experiment, there was less than 0.5% total weight loss and there was no sign of significant reaction with the cell. Those compounds which did appear to decompose to some extent produced final compositions which lie within the $\text{Cd}(\text{OH})_2$ phase region bounded by the diselenide.

In the case of Cr_2Se_3 , the weight loss calculated from the increase in weight of the cell corresponds very closely to formation of the previously reported composition $\text{CrSe}_{1.14}$. However, since there was such a large reaction with the cell, this result should perhaps be considered fortuitous.

For TaSe_2 , the final composition lies within the $\text{Cd}(\text{OH})_2$ phase region but is beyond the phase reported as $\text{TaSe}_{1.98}$. The first dip in the weight curve of experiment M9 was a change of approximately 1.5 weight %. If no weight loss had occurred before this dip then it would correspond to a composition change from $\text{TaSe}_{2.00}$ to $\text{TaSe}_{1.94}$.

Since the extent of decomposition in the effusion cell experiments was so small, the lack of accurate T.G.A. curves probably did not result in the loss of much significant information.

2. Free Vaporization Experiments

Since more reliable T.G.A. curves are available for these experiments and since in general larger degrees of decomposition were observed, each compound will be discussed individually.

(a) TiSe_2 (see Figures 16 and 24, experiments M3 in table 3 and L1 in table 4)

The 3.0% weight loss beginning at 140°C corresponds to the formation of $\text{TiSe}_{1.92}$ from $\text{TiSe}_{2.00}$, but no new phase has been reported at such a composition. A feasible explanation for the dip is that it is due to free selenium in the sample since data quoted by Duval⁽⁶¹⁾ and extrapolated in figure 25 indicate that the vapor pressure of selenium at 143°C is 10^{-4} mm Hg which is approximately the pressure used in the experiments in this study.

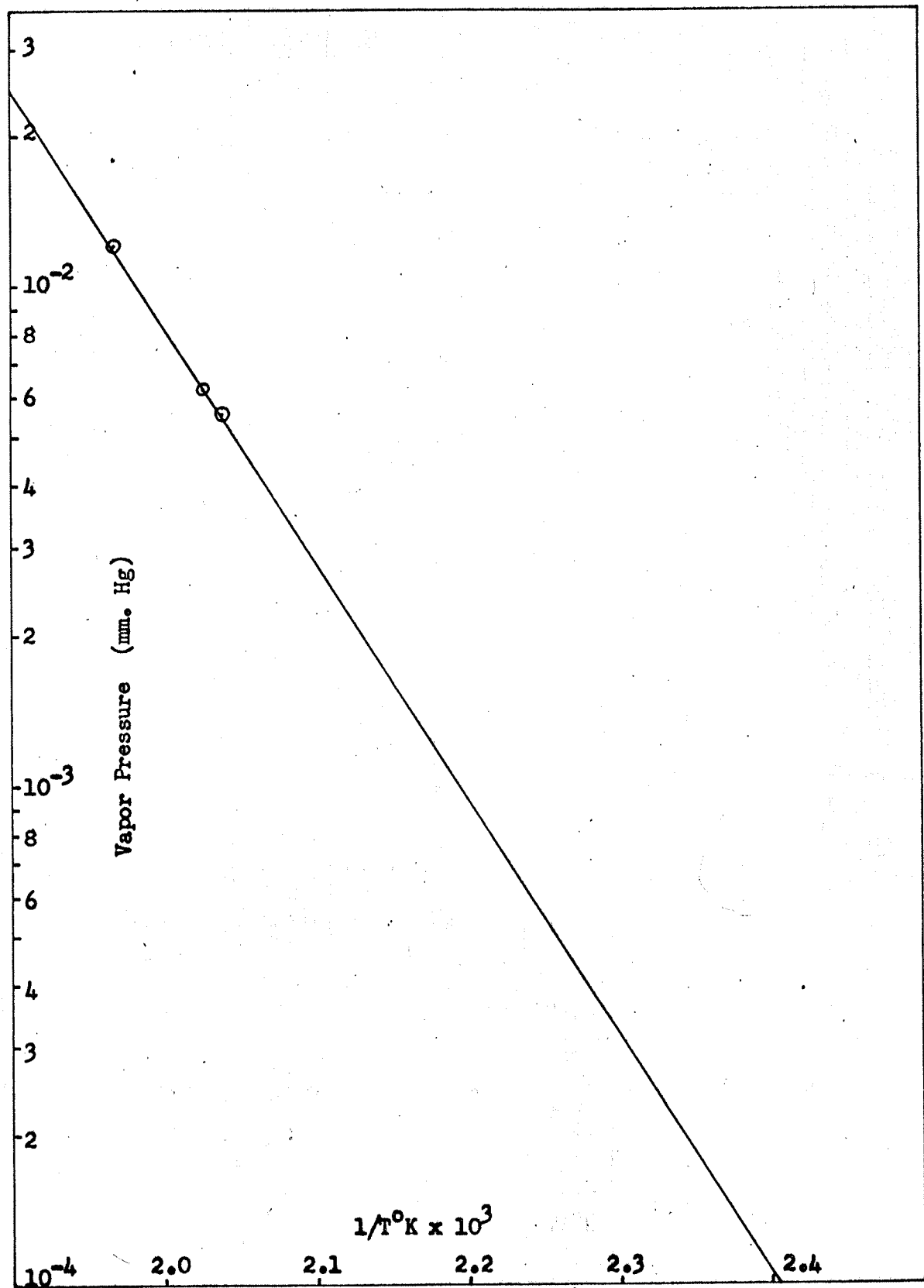
Recalculation of the results of experiment L1 assuming that the original sample consisted of TiSe_2 with 3% of unreacted selenium gives $\text{TiSe}_{1.67}$ as the composition of the final product. Both this composition and the one listed in table 3 lie within the $\text{Cd}(\text{OH})_2$ phase region of the Ti-Se system so that changes of the slope of the weight vs time curve cannot be associated with any reported phases.

FIGURE 25

VAPOR PRESSURE OF SELENIUM

Log P vs. $1/T^{\circ}\text{K}$ extrapolated to 10^{-4} mm. Hg

Data from Pascal(61)



(b) VSe_2 (see figures 17 and 24, experiments M5 in table 3 and L2 in table 4)

The apparent products of both experiments L2 and M5 lie within the $Cd(OH)_2$ phase region.

The only sudden weight change in experiment L2 occurred at $150^\circ C$. This temperature and the small size of the change suggest by the argument used for $TiSe_2$ above that it was due to loss of free selenium. The lack of weight change when the sample was pre-heated in vacuum at $60^\circ C$ in experiment M5 probably indicates that there was not a significant amount of water vapor adsorbed on the sample, but the temperature appears to have been too low to sublime the free selenium in a reasonable amount of time.

(c) Cr_2Se_3 (see figures 18 and 24 and table 4)

Decomposition in experiment L3 begins at $640^\circ C$ and proceeds continuously to $CrSe_{0.78}$. The lack of any sudden changes of slope in the weight curve could be taken as evidence that the three reported phase regions shown in figure 24 are in fact one phase with a continuously changing structure similar to that reported for the Ti-Se system between $TiSe_{1.5}$ and $TiSe_{1.09}$. This suggestion could be tested by examination of the crystal structures of compositions between the three reported phase regions.

The fact that the decomposition continues smoothly to $CrSe_{0.78}$ suggests that the lower end of the NiAs phase,

which is reported as approximately $\text{CrSe}_{1.0}$, may in fact extend to $\text{CrSe}_{0.78}$.

(d) ZrSe_2 (see figures 19 and 24 and table 4)

The results of the free vaporization of this compound are very similar to those obtained for VSe_2 . A small decomposition at 150°C , explainable as loss of free selenium, is followed by a further small decomposition to a product still within the reported $\text{Cd}(\text{OH})_2$ phase region.

(e) MoSe_2 (see figures 20 and 24 and table 4)

There is a small weight loss of 1.3 weight % ending at 150°C which may be due to loss of free selenium. The fact that it began at 60°C may indicate that part of it was due to water adsorbed on the sample. Such an early weight loss was not observed in the case of any of the other samples. However, the MoSe_2 used was in the form of much finer powder than any of the other compounds except WSe_2 .

The weight curve shows a definite change in slope at 84.7 weight % (see point A in figure 20) while the sample is at a constant temperature of 1000°C . This weight corresponds to a composition of $\text{MoSe}_{1.51}$. If the 1.3% weight loss is assumed to be due to some type of impurity and that the remainder of the original sample is MoSe_2 , then the point A would correspond to $\text{MoSe}_{1.52}$. In either case, it seems reasonable to identify the change of slope with the phase which has previously been reported as Mo_2Se_3 .

The change of slope begins at 87.4 weight % and is complete by 82.9 weight %. The fact that it is such a gradual change is considered more likely to be the result of pressure and temperature differences within the powdered sample causing the reaction to be complete at different times in different parts of the sample than a measure of the range of stability of the Mo_2Se_3 phase.

The weight curves on either side of this Mo_2Se_3 phase are linear, indicating constant vaporization rates and hence constant vapor pressures. From phase rule considerations it is reasonable to suggest that each of these constant vapor pressures at constant temperature corresponds to the pressure of a gaseous phase above two condensed phases in equilibrium. Assuming that MoSe_2 is still present after the temperature has reached 1000°C , the condensed phases associated with the first straight line would be MoSe_2 and Mo_2Se_3 . The composition of the final product of experiment L5 was calculated to be $\text{MoSe}_{1.09}$ so that the phases at the ends of the second straight line may be designated Mo_2Se_3 and MoSe . Thus it is suggested that the two regions of constant vaporization rate at 1000°C indicate that the phases MoSe_2 , Mo_2Se_3 and MoSe have narrow regions of homogeneity and are the only stable phases in the Mo-Se system between 66.7 and 52.2 atom percent selenium. This result is in strong contrast with the Ti-Se system which is reported to have

a continuously changing structure between the same composition limits.

(f) TaSe_2 (see figures 21 and 24 and table 4)

By a similar discussion to that given for TiSe_2 above, the small drop in weight at 150°C may be explained as loss of unreacted selenium. The total weight change is small and corresponds to a composition change within the $\text{Cd}(\text{OH})_2$ phase region.

(g) WSe_2 (see figures 22 and 24 and table 4)

This compound showed the greatest degree of decomposition of any of the compounds studied. The constant temperature weight curve seems rather complex, particularly when compared with the lack of reported stable phases in the W-Se system.

There is no feature of the weight curve which can be associated with the $\text{WSe}_{1.95}$ end of the reported phase shown in figure 24. The first discontinuous change in slope after the commencement of decomposition is at 95.2 weight % or $\text{WSe}_{1.73}$ (point A in figure 22). The other points on the curve which might correspond to distinct phases are: $\text{WSe}_{1.29}$ (point B), $\text{WSe}_{0.91}$ (point C), $\text{WSe}_{0.77}$ (point D) and $\text{WSe}_{0.49}$ (point E).

Of the possible phases indicated, the strongest evidence is probably for $\text{WSe}_{0.49}$, or approximately W_2Se , since there appear to be two well defined straight lines

intersecting at this point. No previous report has been found of any phase below WSe_2 in the W-Se system.

CONCLUSIONS

A. All of the compounds studied decompose to some extent in vacuum below 1000° C. The group VIb selenides Cr_2Se_3 , MoSe_2 and WSe_2 are more stable than the diselenides of groups IVb and Vb, the order of thermal stability in group VIb being $\text{MoSe}_2 > \text{WSe}_2 > \text{Cr}_2\text{Se}_3$.

B. The decomposition pressures are of the order of 10^{-4} mm. Hg or less at 1000° C.

C. Evidence was found that at 1000° C:

1. the Cr-Se system contains a region of continuously variable composition between Cr_2Se_3 and $\text{CrSe}_{0.78}$.

2. the phases MoSe_2 , Mo_2Se_3 and MoSe have narrow regions of stability and are the only phases present in the Mo-Se system between 66.7 and 52.2 atom percent selenium.

3. the W-Se system contains a narrow phase at W_2Se and possibly other phase boundaries at $\text{WSe}_{1.29}$, $\text{WSe}_{0.91}$ and $\text{WSe}_{0.77}$. None of these phases have previously been reported.

4. thermal decomposition of the diselenides of Ti, V, Zr and Ta is limited to the $\text{Cd}(\text{OH})_2$ phase region close to the composition MSe_2 .

BIBLIOGRAPHY

- (1) L. H. Brixner, *J. Inorg. Nucl. Chem.*, 24, 257 (1962).
- (2) H. Haraldsen, *Angew. Chem. Internat. Edit.*, 5, 58 (1966).
- (3) A. Kjekshus and W. B. Pearson, "Phases With the Nickel Arsenide and Closely-Related Structures" in *Progress in Solid State Chemistry, Volume 1*, H. Reiss ed., The MacMillan Company, New York, (1964), p. 83.
- (4) F. K. McTaggart and A. D. Wadsley, *Australian J. Chem.*, 11, 445 (1958).
- (5) F. K. McTaggart, *Australian J. Chem.*, 11, 471 (1958).
- (6) F. K. McTaggart and A. Moore, *Australian J. Chem.*, 11, 481 (1958).
- (7) J. Bear and F. K. McTaggart, *Australian J. Chem.*, 11, 458 (1958).
- (8) P. M. Magie, *Lubrication Engineering*, 22, 262 (1966).
- (9) P. Bernusset, *Rev. Chim. Minerale*, 3, 135 (1966).
- (10) P. Bernusset, *Chim. Mod.*, 10, 277 (1965).
- (11) F. M. A. Carpay, *J. Inorg. Nucl. Chem.*, 28, 2827 (1966).
- (12) Von Bolton, *Z. Elektrochemie*, 11, 45 (1905).
- (13) H. Schäfer and W. Fuhr, *J. Less Common Metals*, 8, 375 (1965).
- (14) B. E. Brown and D. J. Beerntsen, *Acta Cryst.*, 18, 31 (1965).
- (15) A. E. Van Arkel, *Physica*, 4, 286 (1924).
- (16) A. E. Van Arkel and De Boer, *Z. Anorg. Chem.*, 148, 345 (1925).
- (17) H. Uelsmann, *Liebigs Ann.*, 116, 122 (1860).
- (18) E. Wendehorst, *Z. Anorg. Chem.*, 173, 268 (1928).
- (19) H. Moissan, *Compt. Rend.*, 90, 819 (1880).
- (20) V. A. Obolonchik and T. M. Mikhlina, *Ukrainskii Khimicheskii Zhurnal*, 30, 1037 (1964).

- (21) E. Eastman, L. Brewer, L. A. Bromley, P. W. Gillies and N. F. Lofgren, *J. Am. Chem. Soc.*, 72, 4019 (1950).
- (22) F. Kadijk, R. Huisman and F. Jellinek, *Rec. des Travaux Chimiques des Pays Bas*, 83, 768 (1964).
- (23) S. S. Sidhu, "Neutron and X-ray Diffraction Studies of Some NiAs-type Structures" in "A Seminar on Groups V and VI Anions," R. J. Beals, J. H. Handwerk and J. F. Schumar, eds., N.A.S.A. Report Number ANL-6855 (1964).
- (24) S. Brunie and M. Chevreton, *Compt. Rend.* 264, 449 (1967).
- (25) H. Hahn and P. Ness, *Z. Anorg. Chem.*, 302, 17 (1959).
- (26) F. Gronvold and F. J. Langmyhr, *Acta Chem. Scand.*, 15, 1949 (1961).
- (27) M. Chevreton and F. Bertaut, *Compt. Rend.*, 255, 1275 (1962).
- (28) P. Bernusset and Y. Jeannin, *Compt. Rend.*, 255, 2973 (1962).
- (29) J. Benard and P. Bernusset, *Z. Anorg. Chem.*, 328, 231 (1964).
- (30) H. Hoschek and W. Klemm, *Z. Anorg. Chem.*, 242, 49 (1939).
- (31) S. Brunie and M. Chevreton, *Compt. Rend.*, 258, 5847 (1964).
- (32) H. Haraldsen and F. Mehmed, *Z. Anorg. Chem.*, 239, 369 (1938).
- (33) M. Chevreton and F. Bertaut, *Compt. Rend.*, 253, 145 (1961).
- (34) M. Chevreton, *Acta Cryst.*, 16, 13 (1963).
- (35) H. Hahn and P. Ness, *Z. Anorg. Chem.*, 302, 37 (1959).
- (36) K. Selte and A. Kjekshus, *Acta Chem. Scand.*, 17, 2560 (1963).
- (37) K. Selte, E. Bjerkelund and A. Kjekshus, *J. Less Common Metals*, 11, 14 (1966).

- (38) E. Revolinsky, B. E. Brown, D. J. Beerntsen and C. H. Armitage, *J. Less Common Metals*, 8, 63 (1965).
- (39) K. Selte and A. Kjekshus, *Acta Cryst.*, 17, 1568 (1964).
- (40) K. Selte and A. Kjekshus, *Acta Chem. Scand.*, 18, 697 (1964).
- (41) E. Revdinsky, G. A. Spiering and D. J. Beerntsen, *J. Phys. Chem. Solids*, 25, 1029 (1965).
- (42) *Chemical and Engineering News*, 39, (34) 37 (1961).
- (43) K. Selte and A. Kjekshus, *Acta Chem. Scand.*, 19, 1002 (1965).
- (44) P. B. James and M. T. Lavik, *Acta Cryst.*, 16, 1183 (1963).
- (45) L. C. Towle, V. Oberbeck, B. E. Brown and R. E. Stajdohar, *Science*, 154, 895 (1966).
- (46) L. A. Aslanov, Y. M. Ukrainskii and Y. P. Simanov, *Zhurnal Neorganicheskoi Khimii*, 8, 1801 (1963).
- (47) E. Bjerkelund, J. H. Fermor and A. Kjekshus, *Acta Chem. Scand.*, 20, 1836 (1966).
- (48) E. Bjerkelund and A. Kjekshus, *Acta Chem. Scand.*, 19, 701 (1965).
- (49) L. A. Aslanov, Y. P. Simanov, A. V. Novaselova and Y. M. Ukrainskii, *Zhur. Neorg. Khim.*, 8, 2635 (1963).
- (50) S. M. Ariya, A. I. Zaslavsky and I. I. Matveeva, "Soviet Research in Crystallography, 1956," Chemistry Collection Series, Consultants Bureau, Inc., New York (1959), p. 5.
- (51) L. Moser and K. Atynski, *Montatsh. Chem.*, 45, 241 (1925).
- (52) N. W. Alcock and A. Kjekshus, *Acta Chem. Scand.*, 19, 79 (1965).
- (53) H. V. A. Briscoe, P. L. Robinson and E. M. Stoddart, *J. Chem. Soc.*, 134, 1439 (1931).

- (54) I. K. Taimni and R. Rakshpal, *J. Praktische Chem.*, 27, 171 (1965).
- (55) P. D. Garn, "Thermoanalytical Methods of Investigation," Academic Press, New York, (1965).
- (56) A. E. Newkirk, *Anal. Chem.*, 32, 1559 (1960).
- (57) An. N. Nesmeyanov, "Vapor Pressure of the Elements," Translated and Edited by J. I. Carasso, Academic Press, New York, (1963).
- (58) J. P. Hirth and G. M. Pound, "Condensation and Evaporation, Nucleation and Growth Kinetics," in B. Chalmers ed., "Progress in Materials Science," V. 11, Pergamon Press, Oxford (1963).
- (59) O. Knacke and I. N. Stranski, *Prog. in Metal Physics*, 6, 181 (1956).
- (60) P. Clausning, *Ann. Physik*, 12, 961 (1932).
- (61) "Nouveau Traité de Chimie Minérale," P. Pascal ed., V. 13, Masson et Cie., 2nd. ed., p. 1692.